Synthesis and Biological Assessment of Silver Nanoparticles Using Adiantum incisum Extracts

Muhammad Aizaz Shuaib
Abdul Wali Khan University Mardan
Waheed Murad
Abdul Wali Khan University Mardan
Asif Khan
State University of Maringá
Sehrish Asad
Abdul Wali Khan University Mardan
Hussan Ara Begum
Abdul Wali Khan University Mardan
Omaish Alqahtani
Najran University
Mohammed A. Alshamrani
Pharmacy College, Umm Al-Qura University
Bassam S. M. Al Kazman
Bsalkazman@nu.edu.sa

Najran University

Research Article

Keywords: Nanoparticles, AgNPs, Biological activities, Optimization, Characterization and extraction

Posted Date: November 10th, 2025

DOI: https://doi.org/10.21203/rs.3.rs-7547333/v1

Additional Declarations: No competing interests reported.

Synthesis and Biological Assessment of Silver Nanoparticles Using *Adiantum incisum* Extracts

Muhammad Aizaz Shuaib[1†], Waheed Murad[1], Asif Khan[2†], Sehrish Asad[1], Hussan Ara Begum[1], Omaish Alqahtani[3], Mohammed A. Alshamrani[4], Bassam S. M. Al Kazman[3*]

1. Department of Botany, Abdul Wali Khan University Mardan, KP Pakistan. aizazkmu@gmail.com (M.A.S), waheedmurad@awkum.edu.pk (W.M), sehrishasad577@gmail.com (S.A), hussanara.begum@gmail.com (H.A.B),.
2. Departament of Technology, Universidade Estadual de Maringa, Umuarama PR 87501-390 Brazil. asif.khan@alumni.usp.br (A.K),
3. Department of Pharmacognosy, College of Pharmacy, Najran University, Najran, Saudi Arabia. osalqahtani@nu.edu.sa (O.A.L.), Bsalkazman@nu.edu.sa (B.S.M.A.K.),
4. Department of Pharmaceutical Sciences, Pharmacy College, Umm Al-Qura University, Makkah 21955, Saudi Arabia. mahshomrani@uqu.edu.sa (M.A.A).

*Correspondence authors: Bsalkazman@nu.edu.sa

† = These authors contributed equally.

Abstract

In this study, we synthesized silver nanoparticles (AgNPs) using methanolic and ethanolic extracts of *Adiantum incisum* and evaluated different biological activities. The transition from bright green to dark brown confirmed the synthesis of AgNPs, which was confirmed by UV-vis spectroscopy absorbance peaks between 400-500 nm. Furthermore, optimized biosynthesis by adjusting different parameters such as temperature, pH, and various salt concentrations. Similarly, the characterization of AgNPs was performed using FTIR, XRD, EDX, and SEM. FTIR revealed the presence of functional groups involved in capping and reduction. XRD confirmed the face-centered cubic crystalline structure, SEM revealed monodispersed spherical particles and EDX confirmed the presence of elemental silver. Similarly, the biological activities of plant extracts and synthesized AgNPs were evaluated. Insecticidal assays against *Tribolium castaneum* demonstrate that AgNPs inhibit more than plant extracts. Phytotoxicity tests against *Lemna minor* indicated that AgNPs possess greater phytotoxic potential and antioxidant activity assessed using the DPPH assay revealed dose-dependent radical scavenging capabilities with AgNPs showing superiority to plant extracts. The analgesic potential was evaluated using the acetic acid-induced writhing test, where AgNPs achieved a higher inhibition rate than extracts. The carrageen-induced paw edema test evaluated anti-inflammatory activity with AgNPs showing greater efficacy. Antibacterial assays against *Shigella dysenteriae* and *Pseudomonas aureginosa* to the antibacterial activity indicated that AgNPs have antibacterial potential. Antifungal activity against *Aspergillus niger* also showed a notable inhibition zone. These findings demonstrate that the biosynthesis of AgNPs from *A. incisum* extracts exhibits significant biological activities, highlighting their potential applications in pharmaceutical and agricultural fields.

Keywords: Nanoparticles, AgNPs, Biological activities, Optimization, Characterization and extraction.

1. Introduction

Nanotechnology operates on the nanoscale and has practical uses in the restructuring or control of matter at the atomic and molecular levels (Nasrollahzadeh et al., 2019). This approach significantly develops pharmaceutics, electronics, cosmetics, diagnostics, water treatment, agriculture (Wang et al., 2024), drug delivery (Sarella et al., 2024), porous textile (Mathew & Paul, 2024), biodiesel production (Panahi et al., 2024), phytoremediation (Sharma et al., 2024) and advanced renewable energy solutions (Simpa et al., 2024). The term "nanoparticle" refers to a material that ranges in size from 1 to 100 nm in size. Holding a nanoscale size delivers advanced qualities, such as high surface-to-volume ratio, high conductivity, high mechanical stability, high optical characteristics, low toxicity, low cost, and relatively simple manufacturing (Moodley et al., 2018). It has several applications in the field of biomedicine. It is typically characterized as the production and use of nanoparticles (NP) (size range of 1-100 nm) in photodynamic therapy (PDT), drug delivery, imaging, biosensing, photothermal treatment (PTT) and other applications (R. Singh, 2019). Since metal and metal oxide nanoparticles offer superior features with a high surface-to-volume ratio and a high dispersion in solution, they have been the subject of a great deal of scientific and technological investigation among all types of NPs (Das Purkayastha & Manhar, 2016).

Among all, silver nanoparticles (AgNP) are unique among metal nanoparticles including Cu, Pd, Au, Ag, Zn, Sn and Co due to their wide range of applications in different sectors including electronic storage systems, diagnostics & treatments, biotechnology, nanomedicine, antimicrobial, food control, textile industry, drug delivery, cosmetic industry, solar cells, water treatment, etc. (Gong et al., 2024; Rafique et al., 2017). Studies have shown that AgNPs possess unique physiochemical properties like, cost effective compared to other metals compared to Au and Pt also having ease of synthesis. AgNP synthesis has a long and well-recorded history dating back more than 120 years. At the start of the 20th century, several chemical and physical processes were employed to produce NPs and increase their efficacy (S. Ahmed et al., 2016). These conventional procedures cannot be considered eco-friendly because they involve the use of costly and toxic chemicals (Vijayan et al., 2016). For the creation of nanoparticles, an alternative green method is used instead of physical and chemical methods (Hebbalalu et al., 2013). Green chemistry is an efficient method to fabricate nanoparticles that reduces the presence of harmful materials and combines cutting-edge technology with a clean and tidy and clean environment (Sahni et al., 2015).

The biosynthetic strategy can be performed using bacteria, algae, fungi, and plants. Plant parts, including roots, stem, leaves, seeds, and fruits, have been used as capping and reducing agents in the production of various nanoparticles because plant extract contains key compounds that function as stabilizing and reducing agents (Narayanan & Sakthivel, 2011).

Today, plants have been used extensively in the synthesis of nanoparticles to overcome the restriction of creating nanomaterials with microbes. Numerous plant species are recognized to be capable of decreasing silver ions and creating silver nanoparticles, including *Trifolium resupinatum*, *Citrus aurantium*, *Aloe vera*, *Jatropha curcas,* and *Solanum melongena* (Logeswari et al., 2013). *Cyclosorus dentatus* and *Nephrolepis biserrata* (Chick et al., 2024), *Gleichenia Pectinata* (Femi-Adepoju et al., 2019), *Histiopteris Incisa* (AP, 2024), *Smyrnium cordifolium* (Rashidi et al., 2024), ferns were known for their ability to reduce silver ions and fabricate silver nanoparticles. Since ancient times, ferns have been known to have both edible and therapeutic uses (Liu et al., 2012). They are rich in phytosterols, carotenoids, polyphenols, and fatty acids. Similarly, many of these substances is also potent antioxidants, which are believed to be crucial to preventing the onset of age-related complications (Farràs et al., 2019). The active component in the plant primarily regulates the synthesis and size of the biosynthesized nanoparticles. Therefore, choosing the right plants to produce nanoparticles is crucial, and due to this, *Adiantum incisum* FORSSK. was selected for the biofabrication of AgNPs.

Adiantum incisum Forssk. (Adiantaceae) is an evergreen fern typically found in the hilly regions of the Murree, Swat and Kashmir areas of Pakistan and is abundantly distributed throughout the world. *A. incisum* is known locally by the names of Mayursikha, Sumble, Hansraj, and Raja hans (Bilal et al., 2022). *Adiantum* species have traditionally been used for respiratory problems such as colds, coughing, fever, pneumonia, and mucus development (Reddy & Day, 2001). The distinctive feature of the plant is its delicate, feathery fronds. The stalk of each frond splits into several smaller stalks called pinnae (Patil et al., 2022). The pinnae of *A. incisum* are small, often rectangular, and have incised border, which gives the fern its local name "Toothed Maidenhair (Irfan et al., 2021). *A. incisum* possess underground rhizomes and have a variety of sizes, but normally the fronds grow to a length of around 20-40 cm (8-16 inches), reproduces through spores that develop on the undersides of the fronds. The current study was designed to synthesize AgNPs and its characterization by various techniques, such as UV, FTIR, XRD, DLS, SEM, and TEM analysis. biofabricated AgNPs were also evaluated for their antioxidant,

insecticidal, phytotoxic, antibacterial, antifungal, analgesic, and anti-inflammatory activities (Asad et al., 2022).

2. Materials and Methods

2.1.Sample Collection and Processing

The specimens (whole plant) *of Adiantum incisum* were collected from the Hills of Thana (34.6309° N, 72.0764° E), 950m elevation from sea level, Malakand District, Khyber Pakhtunkhwa (KP), Pakistan. *A. incisum* a wild medicinal plant available everywhere (March-July), especially in the mountainous/hilly areas and we arranged a study tour along with Professors for its collection, considering wildlife roles and regulations. The collected plant samples were properly identified as '*Adiantum incisum* FORSSK', by Assistant Professor Dr Muhib Shah (Ecologist/Taxonomist), Department of Botany, Abdul Wali Khan University, Mardan, Khyber Pakhtunkhwa, Pakistan and confirmed it with the existing literature (Pandey et al., 2024).

The collected materials were kept properly, pressed and labeled. Similarly, the collected plant material were transferred to the Pharmacology laboratory, at Department of Botany, Abdul Wali Khan University, Mardan, Pakistan and washed extensively with tap water to remove dirt and other silicate particles and allowed to dry in the shade. The collected samples were labeled and submitted to the Herbarium (Awkum. Bot. 2-3(FOC).17.7), Department of Botany, Abdul Wali Khan University, Mardan, KP Pakistan (Irfan et al., 2021).

2.2.Extraction

The shade-dried samples were fine powder using an electric grinder and 200g of fine powder was obtained and stored for further use (Das et al., 2010). Extractions were carried out using methanolic and ethanolic solvents by macerating 50 g of powder in 250 mL flasks of the respective solvents, separately. The mixtures were kept in the shaker for 7 days and filtration was done with three solvent replacements. The crude extracts were placed in a water bath to allow the methanol and ethanol to evaporate. After completion of solvent evaporation, the dried extract of *A. incisum* was used as a capping and reducing agent for the fabrication of AgNP (Leo et al., 2013).

2.3.Biosynthesis of nanoparticles

2.3.1. Preparation of 1mM solution of silver nitrate

Silver nitrate ($AgNO_3$) was delicately weighed (0.0422g) using an electronic balance and a 1mM concentration was obtained by dissolving it in 250 mL of distilled water (Balamanikandan et al., 2015).

2.3.2. Fabrication of AgNPs

Silver nanoparticles (NP) were fabricated by combining $AgNO_3$ solution with methanolic and ethanolic extracts of *A. incisum*. Silver nanoparticles (NP) were created using plant extracts that worked as a reducing, capping, and stabilizing agent in a green chemistry approach (A. Ahmed et al., 2022). A plant extract that includes 200µg/mL was made in 50 mL of distilled water and was subsequently added in dilutions of 1mL to a 1mM AgNO3 solution in ratios of 1:1, 1:2, 1:3, 1:4, 1:5 and 1:6. The mixture was stirred for 24 hours at room temperature until the color of the solution changed to yellowish brown. In comparison to other ratios of the silver nanoparticle solutions, the color of the 1:5 ratio changed more quickly. (Chouhan & Guleria, 2020) and the biosynthesis of AgNP was confirmed through UV-vis spectroscopy.

The biofabricated AgNPs were further polished by repeated centrifugation at 14800 rpm for 15 minutes at 25-30 ° C. After the supernatants, the pellets were redispersed in distilled water. The biosynthesized AgNPs were then vacuum-dried for 24h, following which the silver nanoparticles (AgNPs) were regularly centrifuged to remove contaminants from loose surfaces. The refined silver nanoparticles were preserved in a freezer and then processed with FTIR and XRD to analyze their capping agent, functional group, structure and composition.(Alharbi et al., 2022).

2.3.3. Optimization of silver nanoparticles

The stability and fabrication of silver nanoparticles (AgNPs) were optimized by changing pH, temperature, and salt concentration (Ibrahim et al., 2021).

2.3.4. PH

The impact of pH levels on the AgNPs synthesized with methanolic and ethanolic extracts of *A. incisum* was investigated. The pH was adjusted with hydrochloric acid (HCl) and sodium hydroxide (NaOH) solutions. UV-vis spectrometry was used to estimate the absorbance of pH at different fractions (1-2, 2-3, 3-4, 4-5, 5-6, 6-7, 7, 7-8, 8-9, 9-10, and 11-12) (Sarsar et al., 2014).

2.3.5. Temperature

To study the impact of different temperatures on the biosynthesis of AgNPs with the crude extracts of *A. incisum*. AgNPs were biofabricated using the methanolic and ethanolic extracts of *A. incisum*. For different temperatures, a total of 14 tiny viols were used, and 3 mL of both methanolic and ethanolic NP solutions were added to each viol that was subjected to water bath at different temperatures for 10 minutes. Similarly, the absorbance of methanolic and ethanolic AgNP solutions is measured using UV-vis spectroscopy (Birla et al., 2013).

2.3.6. Salt

To determine the various impacts of sodium chloride (NaCl) on AgNP production with methanolic and ethanolic extracts of *A. incisum*, a 1 mM solution of NaCl was created by dissolving 1.168g of NaCl in 20 mL of distilled water. Additionally, 2 mL of AgNPs solution of methanolic extract was taken (separately) in five viols and 2 mL of AgNP solution of ethanolic extract was added in the other five viols. Subsequently, 1mM NaCl solution was added at concentrations of 0.2, 0.4, 0.6, 0.8 and 1 mL mL in each vial respectively. The resulting solution was analyzed for absorbance using UV spectroscopy (Devi et al., 2017).

2.4.Physical Characterization

2.4.1. UV-vis spectroscopy

AgNPs were made out of silver nitrate and crude extracts of *A. incisum*. Their synthesis was confirmed by ultraviolet-visible (UV-vis) spectroscopy, in which the measured ultraviolet-visible spectrum was compared to the standard. Absorbency measurements of the biofabricated AgNPs were done using distilled water as a blank solution. The AgNPs were monitored with a UV-1602 double beam UV-vis spectrometer that has a resolution of 1nm. The biosynthesized

AgNPs from silver nitrate and methanolic and ethanolic extracts were made in various ratios which include 1:1, 1:2, 1: 3, 1: 4 and 1:5. The mixtures of these nanoparticles were measured at absorbance from 300 to 800 nm (H. Huang et al., 2020).

2.4.2. FT-IR Spectroscopy

The samples were thoroughly dried at 38 ° C in a vacuum drier, after which the silver nanoparticles were incorporated with KBr and compressed into pellets using a hydraulic pellet press. The methanolic and ethanolic extracts of *A. incisum* and associated AgNPs were analyzed using FT-IR spectroscopy. The samples were measured using the "Perkin Elmer Spectrometer FT-IR SPECTRUM ONE' within a range of 4000cm–0cm-1 with a resolution of 4cm-1 (Alharbi et al., 2022).

2.4.3. X-Ray Diffraction (XRD) Analysis

XRD analysis was performed on biofabricated AgNPs of the *A. incisum* methanolic and ethanolic extracts of *A. incisum* using a JEOL JDX 3532 X-ray diffractometer. The diffraction patterns of the biosynthesized silver nanoparticles were examined using a nickel monochromator that filtered Cu-K radiation for a tube current of 30 mA and tube voltage of 40KV. The average diameter of the NPs of highest intensity was computed using the line width of the reflection peak. The Scherr equation was used to compute the size of the AgNPs.

.

$$D = \frac{K\,\lambda}{\beta 1/\,2\cos\theta}$$

The average crystalline domain size parallel to the reflecting planes is denoted here by the letter "D". Shearer K (0.89) with an X-ray wavelength of (= 1.5406A0) and the coefficient FWHM in radius and Bragg angle (Acay et al., 2019).

2.4.4. Scanning electron microscopy and energy-dispersive X-ray analysis

The surface morphology and chemical composition of the biosynthesized AgNPs were investigated using scanning electron microscopy (SEM) and energy-dispersive X-ray analysis

(EDX). The pallet sample for both SEM and EDX analyses was obtained by centrifuging the methanolic and ethanolic NP solutions at 14,000 rpm for 12 minutes. The acquired pellet was redispersed in distilled water and re-centrifuged at the same speed. The AgNPs were then sonicated in distilled water for 10 minutes. A drop of the suspension was placed on a carbon-coated copper grid which was then put under a mercury lamp for curing. It was later inserted into the same equipment (MIRA 3 XM field emission scanning electron microscope (FESEM) for SEM and EDX analysis. Both extracts of *A. incisum* from biosynthesized AgNPs were placed in a vacuum oven and dried at 350 C. A sample of AgNPs was prepared using a low amount of material to a carbon SEM grid and letting it dry, followed by sputtering with silver using an auto fine coater and imaging with the FE-SEM to observe the morphological features (Mofolo et al., 2020).

2.4.5. Energy-Dispersion Spectroscopy

The pallets were collected after centrifuging AgNP solution for 15 minutes at a speed of 14800 rpm. To verify the existence of Ag element in synthesized AgNPs, we analyzed the AgNPs pallets were analyzed using EDS – Energy-Dispersion Spectroscopy. For this analysis, the EDS probe of the mass powder was performed using a thermally triggered EDS connected to an Oxford Inca 200 SEM (Mofolo et al., 2020).

3. Biological Activities

3.1.Antioxidant Activity

The antioxidant activity of AgNPs and crude extracts (methanolic and ethanolic) biosynthesized from *A. incisum* was evaluated using the 1, 1-diphenyl-2-picrylhydrazyl (DPPH) assay (Shehzada, 2018). Various solutions of plant methanolic, ethanolic, and biosynthesized AgNPs at concentrations of 50, 100, and 500µL/mL were placed in separate test tubes to which 2 mL of DPPH solution (which was prepared at 0.004 % w/v) termed stock solution was added to bring the total volume to 3 mL. The resulting solution was then kept for 1 hour of incubation at room temperature in the dark. The degree of radical reduction percentage was measured using a 517-nm spectrophotometer, with DPPH solution set as the standard and ascorbic acid as the positive control. The experiment was carried out in triplicate and the percentage of absorbance was calculated using the formula provided below.

;

$$\text{Antioxidant potential } (\%) = \frac{\text{Absorbance of control (nm)} - \text{absorbance of test (nm)}}{\text{Absorbance of control}} \text{ x } 100$$

3.2.Insecticidal Activity

The insecticidal activity of the methanolic and ethanolic extracts and their respective AgNP of *A. incisum* were tested against *Tribolium castaneum* (Asad et al., 2022) Plant extracts and the AgNPs were prepared in distilled water to make stock solutions (1 mg/mL). The filter paper (9 cm) was cut to the size of the Petri dish and placed inside it. From the stock solution, the following three fractions were made in duplicate: 100, 500, and 1000 µL/mL. The stock solutions were deposited on the filter paper in the Petri dish using autoclaved micropipette tips. The distilled water within the plates was allowed to evaporate by letting them sit unattended for 24 hours at room temperature. Additionally, each Petri plate was separately populated with 10 healthy samples of each insect species (*T. casteneum*) using a sterilized brush. end, all Petri Plates were placed in a growth chamber set at 28 ° C with 55% relative humidity and checked after 24, 48 and 72 hours. The mortality percentage was calculated using the following formula.;

$$\text{Mortality } (\%) = \frac{100 - \text{Number of alive insects in a test}}{\text{Total number of insects}} \text{ x } 100$$

3.3.Phytotoxic Activity

Lemna bioassay techniques were used to evaluate the phytotoxic effects of biofabricated AgNPs and plant extracts methanolic and ethanolic (Sultana et al., 2019). The experiment was carried out using two replicates for each of the three concentrations (50, 100, 500µL/mL) in the Petri dishes. A stock solution was prepared by adding 1 mL of extract to 1 mL of distilled water and thereby dissolving it, yielding a solution of 1000 ppm. Subsequently, three concentrations of 50, 100, and 500µL were created from the original 1000ppm solution. The stock solution (1mg/ml) of the plant extracts and their AgNPs was prepared in distilled water. Then the E medium was transferred to autoclaved Petri plates to aid in the growth of *Lemna minor* L. Different sample dilutions, that is, 50, 100 and 500µl) were transferred to Petri dishes containing E medium and the final dilution became 15 mL in each petri dish. As a reference growth inhibitor, atrazine was used as a negative and positive control. Eventually, 10 healthy *L. minor* plants, each with three fronds,

were placed inside the Petri dishes and incubated for seven (7) days at 28 ° C. After incubation, the percentage (%) was monitored by using the formula;

$$\text{Inhibition (\%)} = \frac{\text{No of fronds in test}}{\text{No of fronds in control}} \text{ x } 100$$

3.4.Anti-inflammatory activity

The anti-inflammatory potentials of the methanolic and ethanolic extracts and biofabricated AgNP of *A. incisum* were checked, following the carrageenan paw edema method in albino mice. Model mices were obtained from the VRI (https://www.asti.cgiar.org/pakistan/directory/veterinary-research-institute-vri-peshawar), located in Peshawar, KP, Pakistan. A total of six (6) groups were made, each having three mice. Group 1st was assigned as the control group and given a regular saline solution. Similarly, group 2nd received 150mg/kg aspirin and was considered the standard group. Mice in groups 3rd and 4th were assigned for the methanolic extract and its silver nanoparticles and received their treatment respectively. Groups 5 and 6th were administered ethanolic extract and its biofabricated AgNP solutions at 3 different doses of 100, 200 and 300 mg/kg. The size of each mouse paw was measured before dose injection and then 10% carrageenan was injected into the right hind paws of mice from groups 2nd, 3rd, 4th, 5th and 6th. One hour after the carrageenan injection, the edema was quantified. After administering the standard drug (aspirin) and different treatment doses, edema was quantified every hour for three hours (Lu et al., 2025). The percentage (%) of anti-inflammatory potential for all samples was calculated with the formula below;

$$\text{Percentage inhibition (\%)} = \frac{Vc - Vt}{Vc} \text{x } 100$$

Where; 'Vc' increase in paw volume in the control group, followed by an increase in paw volume in animals treated with plant extract and their AgNPs are indicated by 'Vt'.

3.5.Analgesic activity

AgNPs and plant extract (methanolic and ethanolic) were evaluated for their analgesic potential in albino mice following an acetic acid-induced writhing method. A total of six (6) groups were formed and each group was represented by three healthy albino mice (30–40g) independent of their sex. Among all, the 1st received 1 mL of normal saline (1% v/v) as they were taken as the control group and the mice of the 2nd group were taken as the disease group and received an acetic

acid solution. Similarly, to other groups i.e. 3rd, 4th, 5th and sixth 1mL acetic acid solution was administered. Acetic acid induces writhing, which was observed after five minutes of injecting the acetic acid solution. After counting the second group was treated with 1 mL of a paracetamol solution (standard). Similarly, methanolic and ethanolic extracts and their biofabricated AgNP solution were given to the fourth, fifth, and 6th groups at various concentrations, that is, 50, 100 and 500 mg/kg respectively (M. Khan et al., 2018). Calculating the percentage (%) of the analgesic potential of all samples was done with the help of the following formula;

$$\text{Inhibition (\%)} = \frac{\text{Writhing numbers in experiment group}}{\text{Writhing numbers in the control group}} \text{ x } 100$$

3.6.Antibacterial activity

The antibacterial property of plant extracts and biosynthesized AgNPs was evaluated by the disc diffusion method. This experiment was performed at the Plant-microbe Interaction Laboratory of the Department of Botany, AWKUM. Two representative bacterial strains, *Shigella dysenteriae* and *Pseudomonas aeruginosa*, were cultured for 12-24 hours to rehydrate them in nutrient broth. Both strains of *P. aeruginosa* and *S. dysenteriae* were grown in nutrient agar medium. Plant extracts and AgNPs were evaluated for their antibacterial properties using the Kirby-Bauer (disc diffusion method). A stock solution of plant extracts and AgNP was prepared in distilled water at different concentrations, such as 25, 50 and 100µL/mL. After being sterilized, the nutrient agar medium was poured into sterilized petri plates and allowed to solidify. Using a micropipette, 10µl of the bacterial solution was added to the solidified medium and the suspension was then distributed using a glass spreader. Four wells with diameters of 0.5 cm were bored in each corner of the petri dish and the sample for the experiment was introduced into these wells. Streptomycin (standard antibiotic) was used as the positive control and distilled water was used as the negative control. The Petri dishes were placed in the incubator at 26 $^{\circ}$C for 24 hours. The antibacterial activity of Ag-NPs was determined by measuring the zones of inhibition using a standard-supplied chart (Keshari et al., 2020).

3.7.Antifungal activity

The antifungal activity of the plant extract (methanolic and ethanolic) and biosynthesized AgNPs was evaluated using the agar well diffusion technique. In addition, to promote fungal

348 growth, aseptic Sabouraud Dextrose Agar (Sigma Aldrich, Germany) was prepared in sterilized
349 test tubes. All materials (PDA) needed for the experiment were placed in an autoclave for one hour
350 at 121 ^{0}C and 17 Ib pressure for maximum sterilization. The medium was poured into Petri dishes
351 and allowed to solidify. The fungal culture was added to the solidified medium with the help of a
352 glass spreader and micropipette containing 10µL of fungal culture. Each Petri dish was marked
353 with a sterile borer, making four 5mm wells. To the wells, labels were assigned; Plant Extracts
354 (PE), NPs, positive control (C^{+}) and negative control (C^{-}). Different amounts (25, 50, and 100µL)
355 of silver nanoparticles and plant extracts (methanolic and ethanolic) were poured into their
356 respective wells. The standard antifungal drug clotrimazole was used as a positive control and
357 distilled water was used as a negative control. Each Petri dish was incubated at 26^{0}C for three days.
358 After three days, the antifungal potency of AgNPs and plant extract was evaluated by measuring
359 the inhibitory zone using a standard scale (Shahzadi et al., 2019).
360
361 *3.8.Statistical analysis*

362 In the current study, all experiments were carried out in triplicate and data were analyzed
363 using one-way analysis of variance (ANOVA), followed by Dennett's test for multiple
364 comparisons. Treatments were compared with their control groups with statistical significance at
365 $p < 0.05$. Similarly, the graphs were prepared using GraphPad Prism and Origin V. 7.5 software.
366
367 **4. Results**
368 *4.1.Biosynthesis of Silver Nanoparticles*

369 The plant extracts (methanolic and ethanolic) were dissolved in the aqueous $AgNO_3$
370 solution. The reaction solution changed from pale green to reddish brown due to activation of the
371 surface Plasmon vibration of AgNPs (**Figures 1 A and B**), suggesting that the silver ions were
372 reduced to AgNPs. A distinct change in color occurred after 20 minutes of continuous stirring and
373 a complete reduction was observed after 24 hours of continuous stirring. The formation of AgNPs
374 was tracked by spectrophotometry, with a frequency range between 300 and 800 nm. A
375 characteristic absorption peak was observed between 400 and 450 nm.

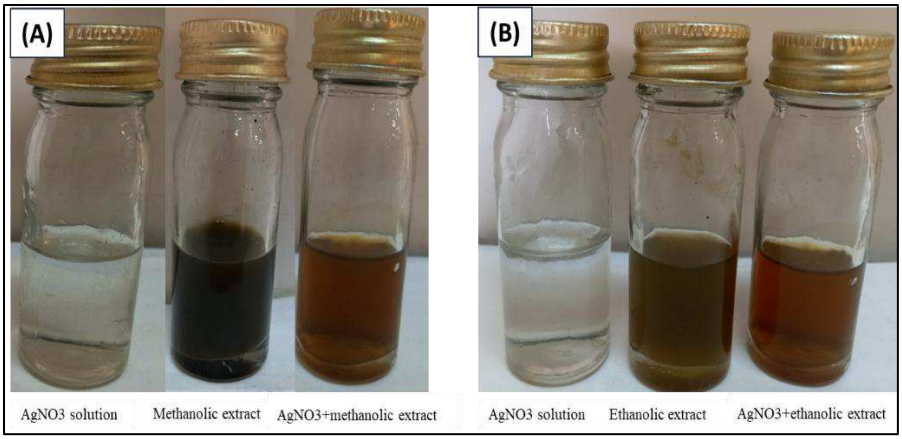

Figure 1; Biosynthesis of AgNO3 nanoparticles from ethanolic and methanolic extracts of *A. incisum*. Where, (**A**) AgNO3 solution + methanolic extract + Methanolic nanoparticles (**B**) AgNO3 solution + ethanolic extract + Ethanolic nanoparticles.

4.2.Optimization of Silver nanoparticles

4.2.1. Effect of pH

The pH range evaluated for the synthesized AgNPs was between 1.0-12.0, and the AgNPs derived from the optimum pH for the methanol extract were between 9.0-10.0. AgNPs were found to be stable under slightly basic and neutral conditions (**Figures 2A and B**). However, the stability diminished when the pH was reduced to 6.0. Higher pH values resulted in higher absorption with narrower peaks. The pH values suggest that both the AgNPs from the methanolic and ethanolic extract were stable between 9-10, with pH 9 supporting maximum stability. These results suggest rapid formation of AgNPs under neutral and basic conditions.

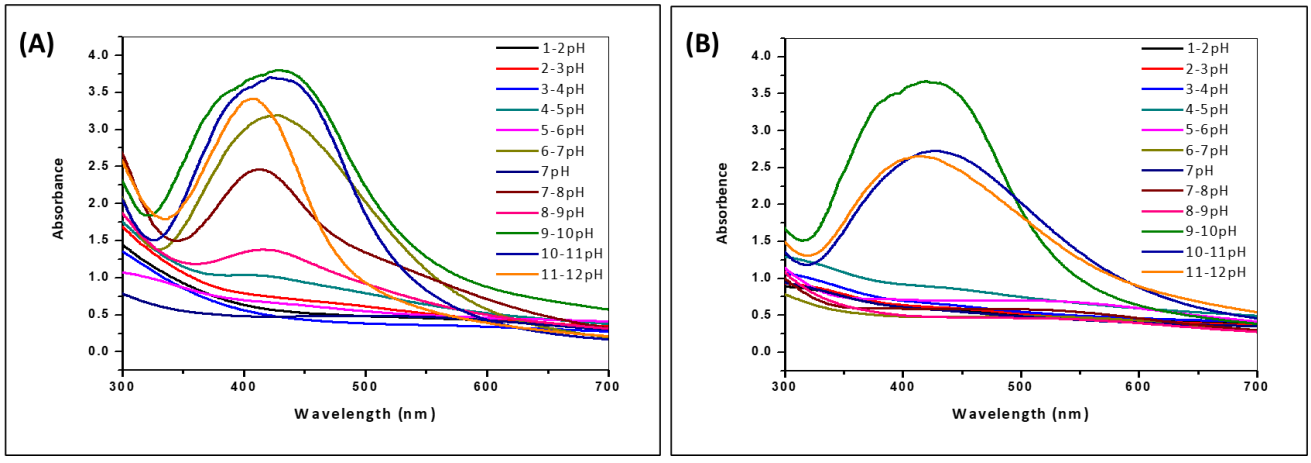

Figure 2: (**A**) UV-UV spectroscopy of the effect of pH on AgNPs synthesized from methanolic extract of *A. incisum* (B) UV-UV spectroscopy of the effect of pH on AgNPs synthesized from ethanolic extract of *A. incisum.*

4.2.2. Effect of Temperature

The influence of temperature on the biosynthesis of silver nanoparticles (AgNP) using methanolic and ethanolic extract of *Adiantum incisum* was studied at 35°C, 50°C, 65°C, 80°C and 95 ° C. It was observed that the optimal temperature for the synthesis of AgNP methanolic extract was around 50–65°C and then reduced when the temperature increased above 65 ° C. These results confirmed that 50 ° C was the optimal temperature for methanolic extracts (**Figures 3A and B)**. Similarly, the fabrication of silver nanoparticles (AgNPs) occurs at a sluggish pace, resulting in nonuniform nanoparticles at room temperature. However, the optimal temperature range of 50 to 65 ° C significantly increases the reaction kinetics. Beyond 65 ° C, the proteins and other biomolecules present in the methanolic extract of *A. incisum* undergo significant thermal denaturation, which further escalates the reduction of the nanoparticles, compromising the stability of the formed nanoparticles.

Similarly, UV spectroscopy absorption spectra demonstrated that ethanolic extract-AgNPs had a maximum absorbance peak at 35 ° C. There was a further drop in absorbance during AgNP formation, when the temperature increased from 35 ° C to 95°C, as indicated in (**Figure 3D**). The results suggest that the ideal temperature for the synthesis of ethanolic extract-AgNP is 35°C. This decrease in the absorbance peak of AgNPs at higher temperatures is most likely due to the fact that the biomolecules from the *A. incisum* extract undergo denaturation.

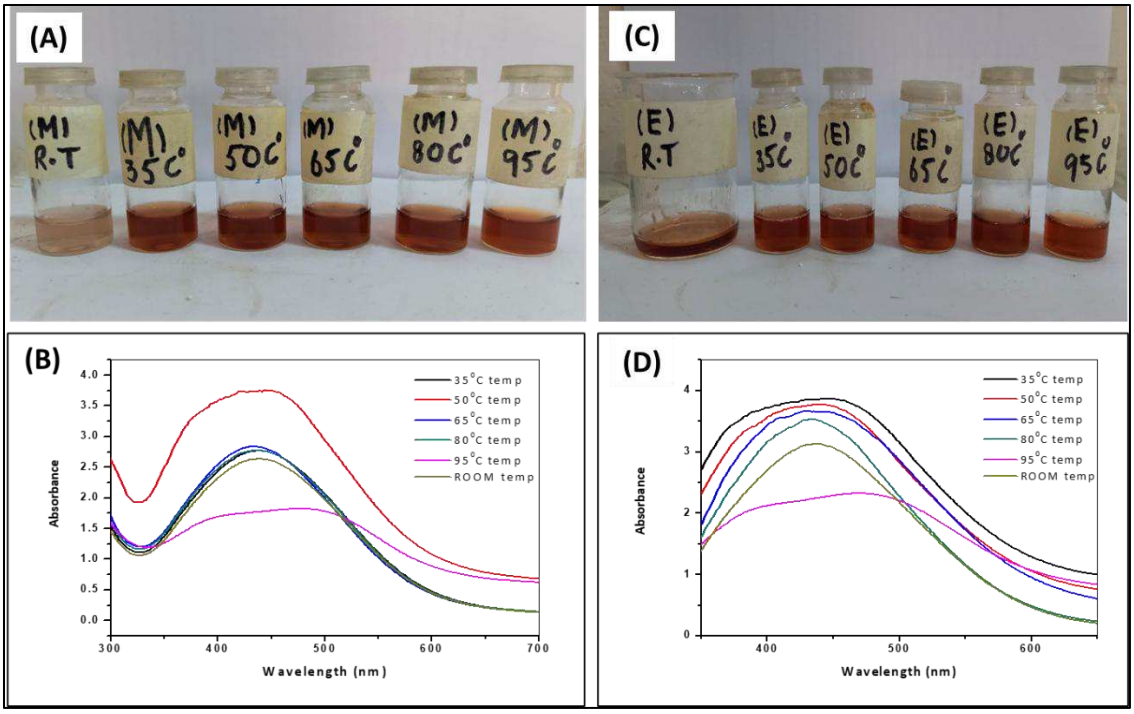

Figure 3: (A) Samples of AgNPs of methanolic extract at different temperatures (B) UV- - spectroscopy of the effect of temperature on AgNPs synthesized from the methanolic extract of *A. incisum* (C) Samples of AgNPs of ethanolic extract at different temperatures (D) UV-spectroscopy of the effect of temperature on AgNPs of ethanolic extract of *A. incisum.*

4.2.3. Effect of NaCl Concentration

The concentration of NaCl is critical in the definition of the shape and size of AgNPs. In the study, the effect of NaCl concentration on the reduction of silver ions was evaluated using UV-vis spectroscopy **(Figures 4AB).** AgNPs were synthesized using Adiantum incisum methanolic and ethanolic extracts, and various concentrations of 1 mM NaCl solution (0.2, 0.4, 0.6, 0.8, and 1 mL) were added to these nanoparticle solutions. The results indicated that AgNPs synthesized from the methanolic extract exhibited a higher absorbance at all tested concentrations but maximum maxima were observed at 0.2mL of NaCl concentration solution. However, with increasing salt concentration, a consistent decrease in absorbance was observed, reaching the lowest value at 1 mL of NaCl.

In addition, UV-vis spectroscopy analysis on the AgNPs produced from the ethanolic extract showed considerable absorbance at all tested NaCl concentrations, with the highest absorbance peak observed at 0.2 mL of salt solution. Higher concentrations of salt led to decreased

formation of nanoparticles. It can be concluded from the findings that for the production of silver nanoparticles using A. incisum methanol and ethanol extracts, the highest peak absorbance occurs at a concentration of mL 0.2mL of salt solution.

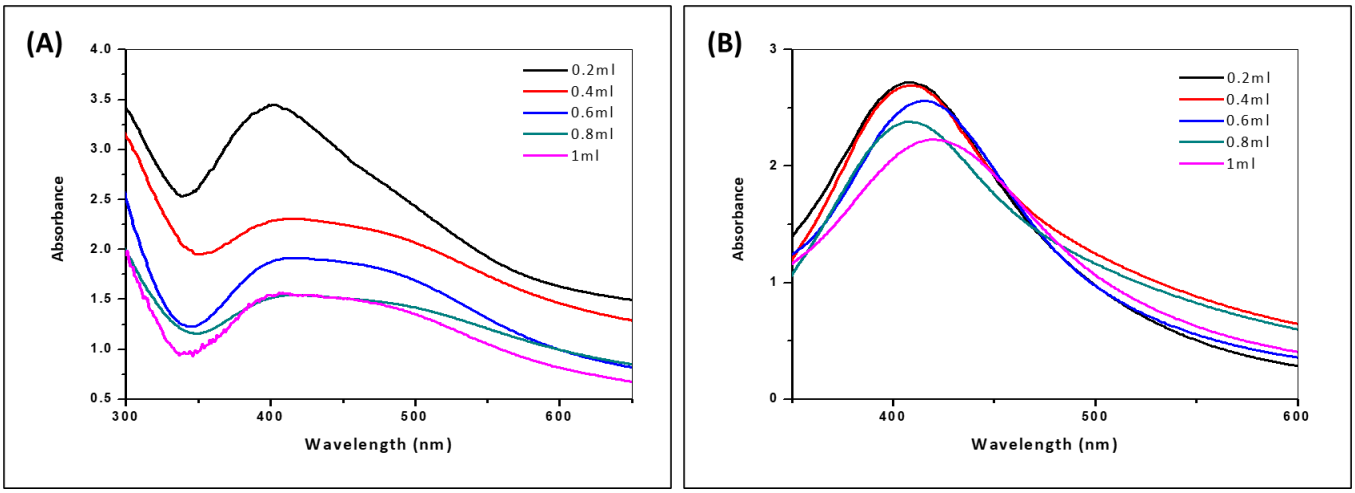

Figure 4: (A) UV-Spectroscopy of the effect of NaCl on AgNPs of the methanolic extract of *A. incisum and* (B) UV-Spectroscopy of the effect of NaCl on AgNPs of the ethanolic extract of *A. incisum.*

4.3.Characterization of silver nanoparticles

4.3.1. UV-vis spectroscopy

UV-visible spectroscopy is considered an advanced form of colorimetry because it follows the basic principle of light absorption from test samples. Spectroscopy offers improved accuracy at wavelengths between 190–700 nm, which is selected as silver nanoparticles (AgNPs) typically show absorbance peaks within this range **(Figure 5AD)**. In this study, a spectrophotometer (300 Plus Optima, Japan) was used in conjunction with quartz cells and 1 mL of distilled water was put as blank. The color change was indicative of the formation of AgNPs, and the synthesis was further confirmed by scanning the absorbance from 200-800 nm. The spectral bands of plant-extract-mediated AgNPs suggest changes in the size and morphology of nanoparticles.

Absorbance tests of the reaction solution containing methanolic extract of A. incisum and 1 mM aqueous silver solution confirmed AgNP formation. Analysis of the absorbance of AgNPs synthesized from methanolic and ethanolic extracts was done in different extract to silver solution ratios which were 1:1, 1:2, 1:3, 1:4 and 1:5. AgNPs mediated by methanolic and ethanolic extracts showed the highest absorbance peak at a 5: 1 ratio and in the wavelength range of 400-500 nm.

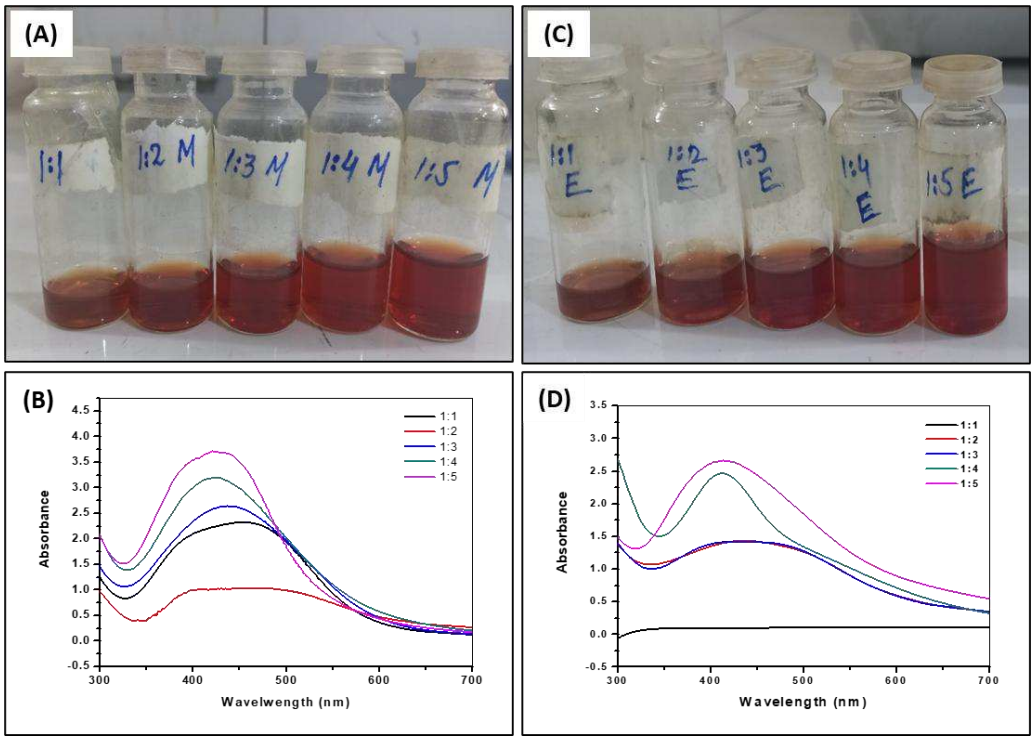

Figure 5: (A) Samples of nanoparticles of methanolic extract in different ratios (B) UV-vis spectroscopy of AgNPs synthesized from methanolic extract of *A. incisum* (C) Samples of nanoparticles of methanolic extract at different ratios (D) UV-vis Spectroscopy of AgNPs synthesized from the ethanolic extract of *A. incisum.*

4.3.2. FT-IR analysis

Fourier transform infrared (FTIR) spectroscopy has been widely applied to study the interactions between capping agents and nanoparticles to validate the functional groups involved in the synthesis of nanoparticles. In this study, FTIR was performed to analyze the primary phytochemicals in the methanolic and ethanolic extracts of *A. incisum* that were responsible for the reduction, stabilization, and capping of biosynthesized silver nanoparticles (AgNP). The FTIR spectra of the extracts and their corresponding AgNP were obtained in the range of 500–4000 cm -1. The data revealed that the AgNPs derived from the methanolic extract presented a distinct peak at 3298 cm^{-1}, which is associated with the amine N-H group, while the peak at 2922 cm -1 was due to the C-H group. There were also shifts at 1493 cm -1cm -1 and 1066 cm^{-1} that were linked to the functional groups C = C and CO, respectively **(Figure 6A).**

FTIR analysis was performed on silver nanoparticles synthesized with the ethanolic extract of *A. incisum*. The IR spectrum exhibited a clear peak at 3364 cm -1 due to the functional group, while the 2921 cm^{-1} peak was associated with the C-H bond These results suggests that these functional groups participated in the reduction and stabilization of AgNP **(Figure 6B).**

.

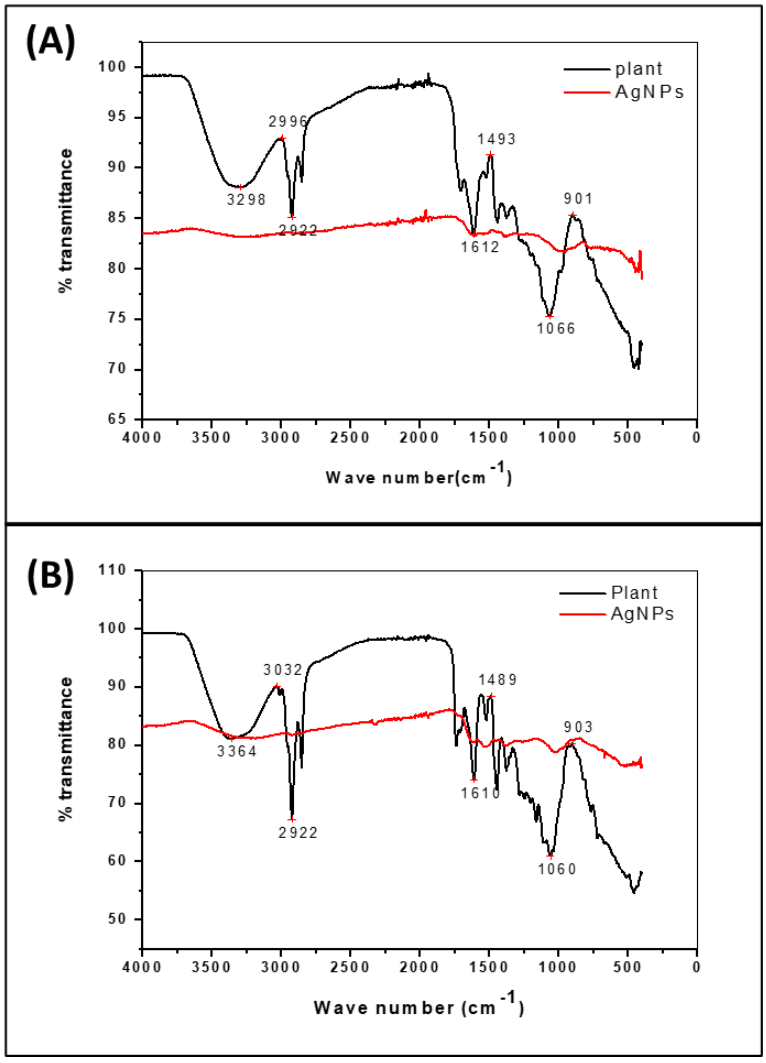

Figure 6: (A) FT-IR of AgNPs and methanolic extract of *A. incisum;* (B) FT-IR of AgNPs and ethanolic extract of *A. incisum* and ethanolic extract of *A. incisum.*

4.3.3. X-Rays Diffraction

XRD analysis was conducted to verify the purity and crystalline structure of silver nanoparticles (AgNPs) synthesized using *the* methanolic and ethanolic extracts. The XRD pattern for AgNP mediated by methanolic extract showed clear peaks at 38.12°, 45.92°, and 64.54 ° that matched the (111), (200), and (220) crystal planes (111), (200) and (220), respectively **(Figure 7A).** These peaks verify the crystalline nature of the synthesized AgNPs.

The XRD study of synthesized biofabricated AgNPs showed distinctive peaks at diffraction angles 37.88º, 46.16º and 76.51º corresponding to the planes (111), (200), and (311), respectively. (**Figure 7B**). It was also observed from the XRD pattern that the AgNPs had a face-centered cubic structure (fcc). The peaks also matched well with the standards of JCPDS file 040783 for silver, which is indicative of the crystalline characteristics of AgNPs synthesized using methanolic and ethanolic extracts of *A. incisum*.

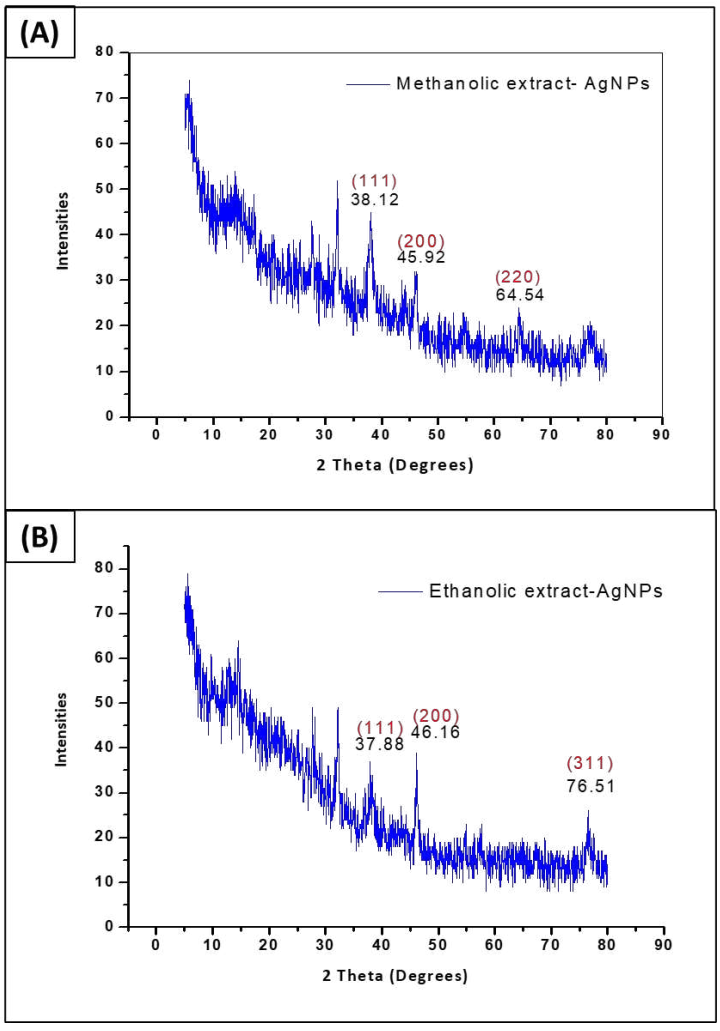

Figure 7 (A) XRD of AgNPs synthesized from the methanolic extract of *A. incisum* (B) XRD of AgNPs synthesized from the ethanolic extract of *A. incisum.*

4.3.4. Scanning electron microscopy (SEM)

SEM was performed to study the structure, form and surface features of silver nanoparticles synthesized using methanolic and ethanolic extracts of *A. incisum* at various magnifications **(Figure 8A-D).**

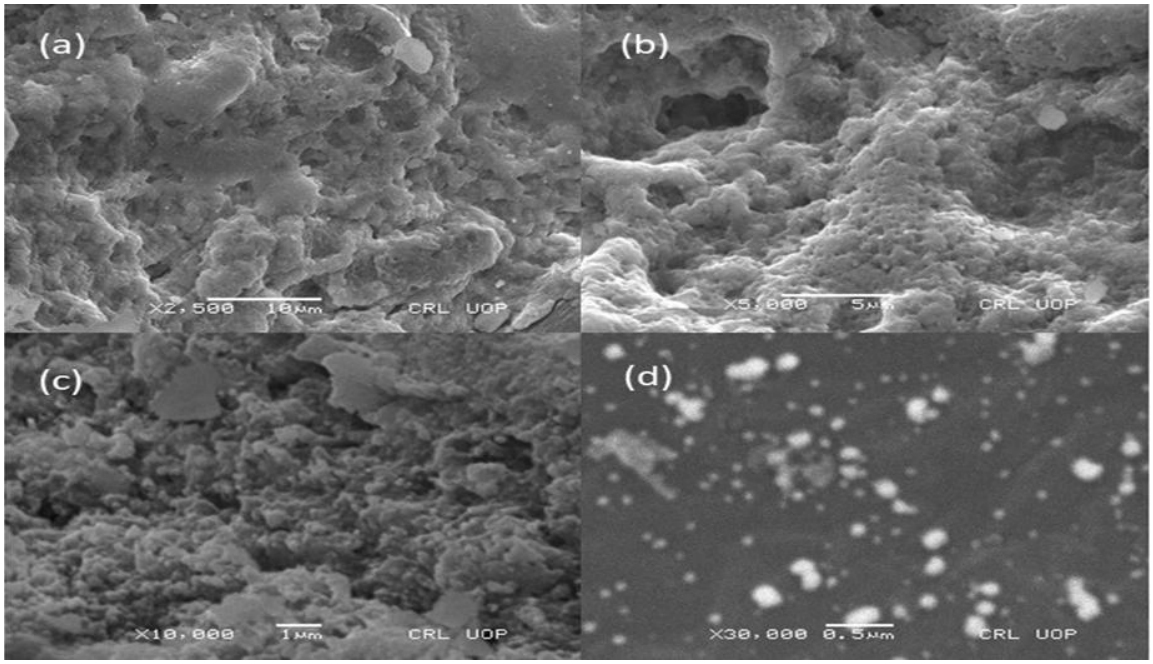

Figure 8: Micrographs of AgNP SEM analysis of methanolic extract at (a)10 µm (b) 5µm (c)1 µm (d)0.5 µm magnifications.

SEM micrographs of the ethanolic extract AgNPs and methanolic extract-AgNPs showed that the nanoparticles were mainly circular, monodispersed, and uniformly dispersed. However, a certain amount of particle agglomeration was observed **(Figure 9A–D).**

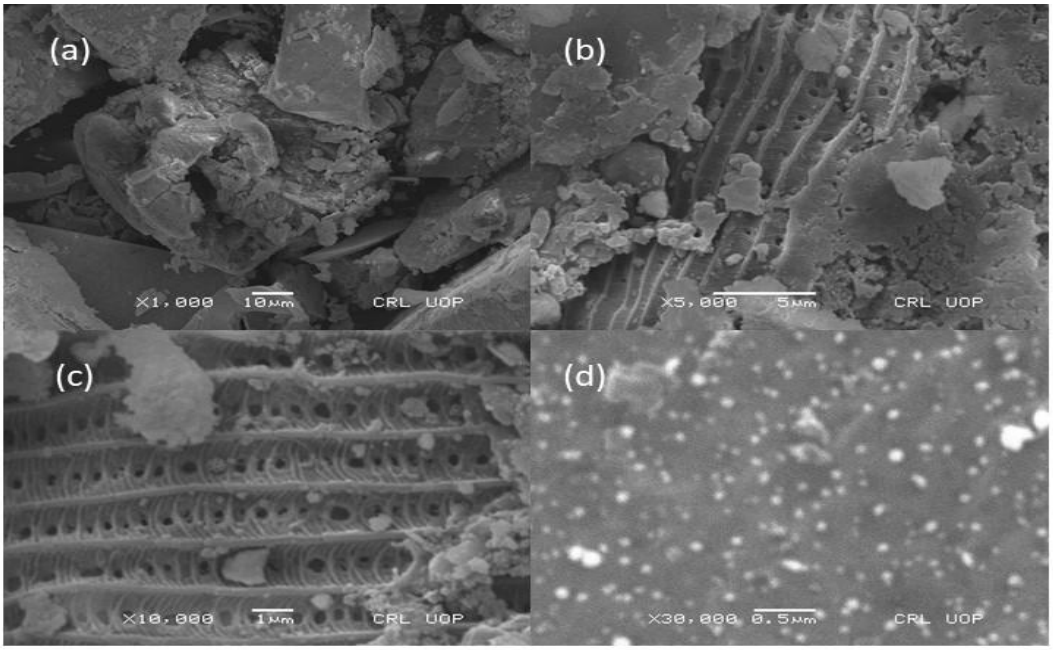

Figure 9: Micrographs of SEM analysis of ethanolic extract AgNP at (a)10 µm (b) 5µm (c)1 µm (d)0.5 µm magnifications.

.

4.3.5. Energy Dispersion Spectroscopy

Energy dispersive spectroscopy (EDS) analysis was done to identify the elemental composition of silver nanoparticles (AgNP) fabricated using methanolic and ethanolic extracts of *A. incisum* **(Figure 10A-B)**. The analysis detected the signal corresponding to Ag at 3 Kev for both the methanolic extract AgNPs and the ethanolic extract AgNPs. Additionally, some other elements such as C, O, Si, and Cl were present in higher amounts in the ethanolic extract-AgNPs, while C and Cl were present in the methanolic extract-AgNPs. The EDS analysis clearly showed the highest peak for Ag, while the peaks for C, O, Si, and Cl were rather modest.

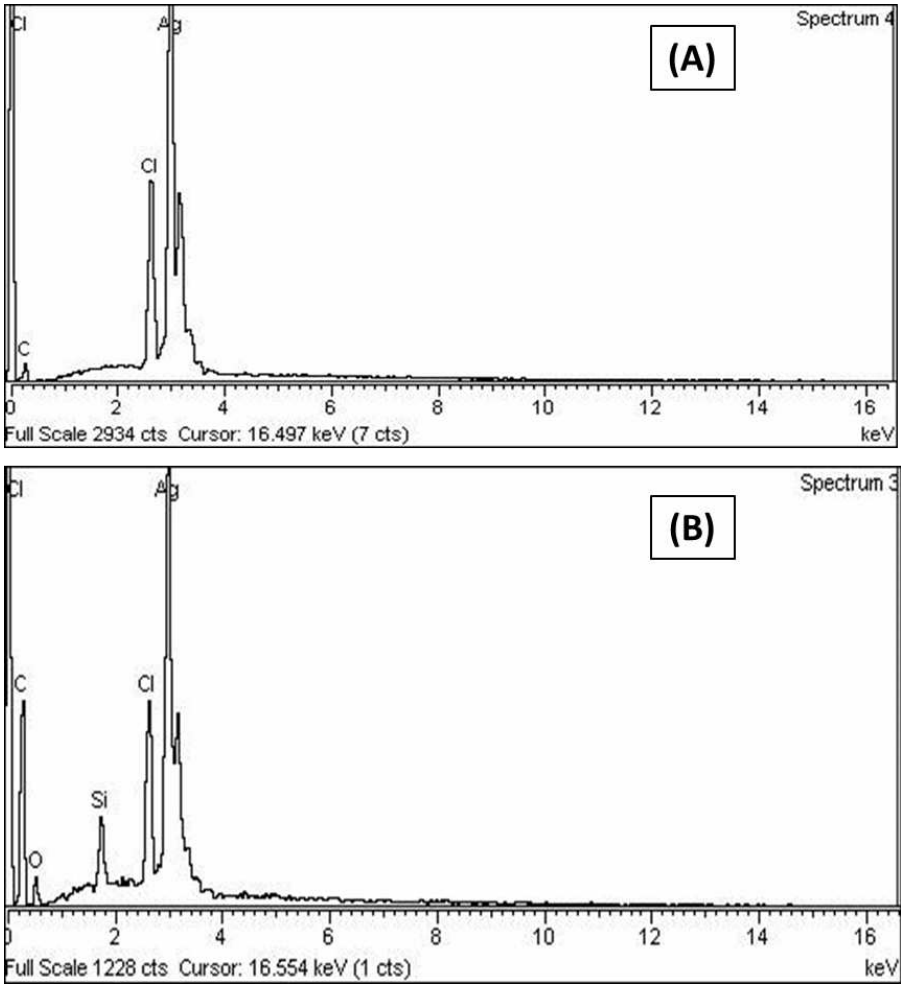

Figure 10: (A) Energy dispersion spectroscopy of methanolic extract-AgNPs, (B) Energy dispersion spectroscopy of ethanolic extract-AgNPs.

4.4. Biological Activities

4.4.1. Antioxidant Activity

The DPPH radical scavenging capacity of methanolic and ethanolic extracts and those derived from *A. incisum*. AgNPs synthesized from ethanolic extract (ENP) showed the highest DPPH radical inhibition at 85.2% (p<0.619) at 500µg/mL (**Figure 11**). After ethanolic nanoparticles, ascorbic acid showed a maximum inhibition of 78.9% at 500 µg/ml, exhibiting significant action (p<0.001), followed by AgNPs synthesized from methanolic extract (MNPs) showed the highest inhibition rate of 64.96% (p<0.626) at 500µg/m. Similarly, ethanolic plant

extract (EPE) and methanolic plant extract (MPE) also showed inhibition of 35.5% and 62.2%, respectively, at 500µg/mL.

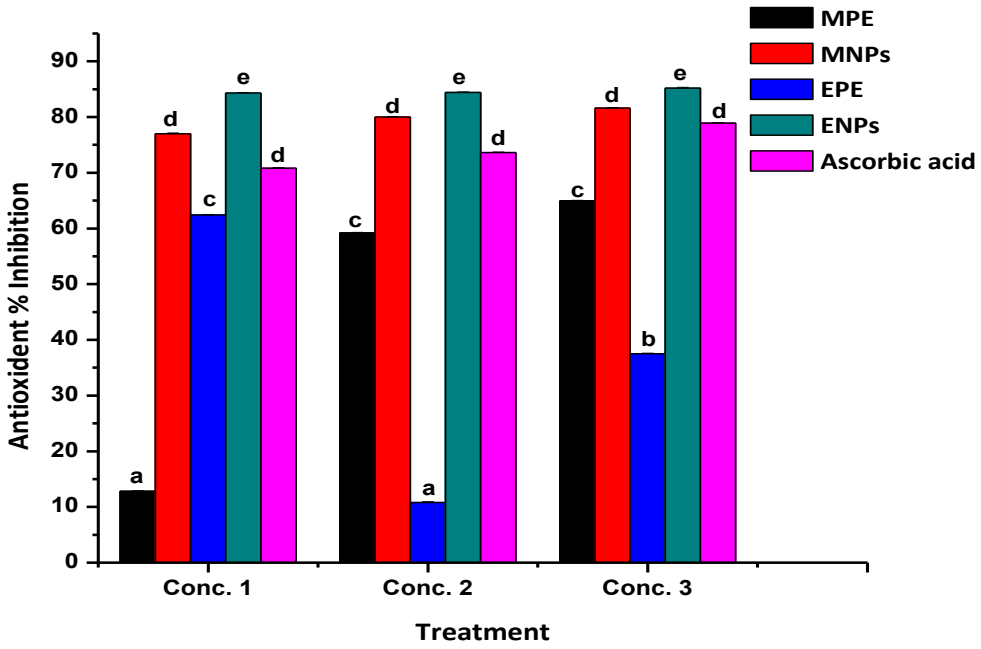

Figure 11: Antioxidant activity of methanolic extract AgNP, ethanolic extract-AgNPs, methanolic and ethanolic extract of *A. incisum* and Ascorbic acid.

4.4.2. Insecticidal Activity

The insecticidal activity of biosynthesized silver nanoparticles from extracts of methanolic (MNP) and ethanolic (ENPs) extracts of *A. incisum* was tested for insecticidal activity on *Tribolium castaneum* **(Figure 12).** The findings revealed that AgNPs had more insecticidal activity than the crude extracts of plants. Methanolic nanoparticles (MNP) exhibited a mortality rate of 56.7% (p<0.576) at 1000 µg/mL, followed by ethanolic nanoparticles (ENP) with a statistically significant mortality rate of 53.4% (p<0.001) at the same concentration. Interestingly, methanolic nanoparticles (MNPs) also showed similar inhibition at 500 µg/mL. The ethanolic plant extract (MPE) led to a mortality of 43.3% (p<0.054) at 1000 µg/mL and the ethanolic plant extract (EPE) exhibited a mortality of 36.7% at the same concentration.

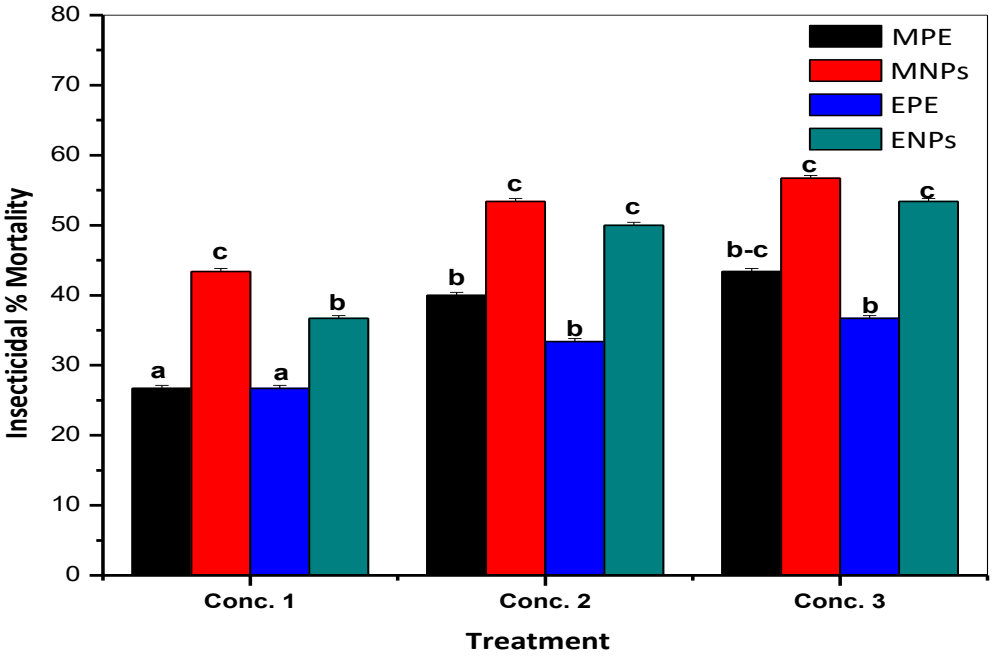

Figure 12: Insecticidal activity of methanolic extract-AgNP, ethanolic extract-AgNPs, methanolic and ethanolic extract of *A. insicum.*

4.4.3. Phytotoxic Activity

The phytotoxic potential of the methanolic and ethanolic extracts of *A. incisum* and their respective AgNPs were examined at concentrations of 50, 100, and 500 g/mL against *Lemna minor* (**Figure 13**). Interestingly, all samples greatly mitigated Lemna minor. Atrazine (common herbicide) was found to show a nonsignificant inhibition of 90% at 1000 µg/mL, followed by ethanolic silver nanoparticles (ENPs) which significantly (p<0.001) revealed 51.11% inhibition at 1000 µg/mL. The result also revealed that the AgNP methanolic extract (MNP) revealed significantly (p<0.001) 45.5% at 1000 µg/mL. The result also showed that the ethanolic plant extract (EPE) had a significant (p<0.001) 36.66% inhibition rate at 1000 µg/mL, while the methanolic plant extract (MPE) showed a significantly significant 35.5% inhibition rate significantly (p<0.001).

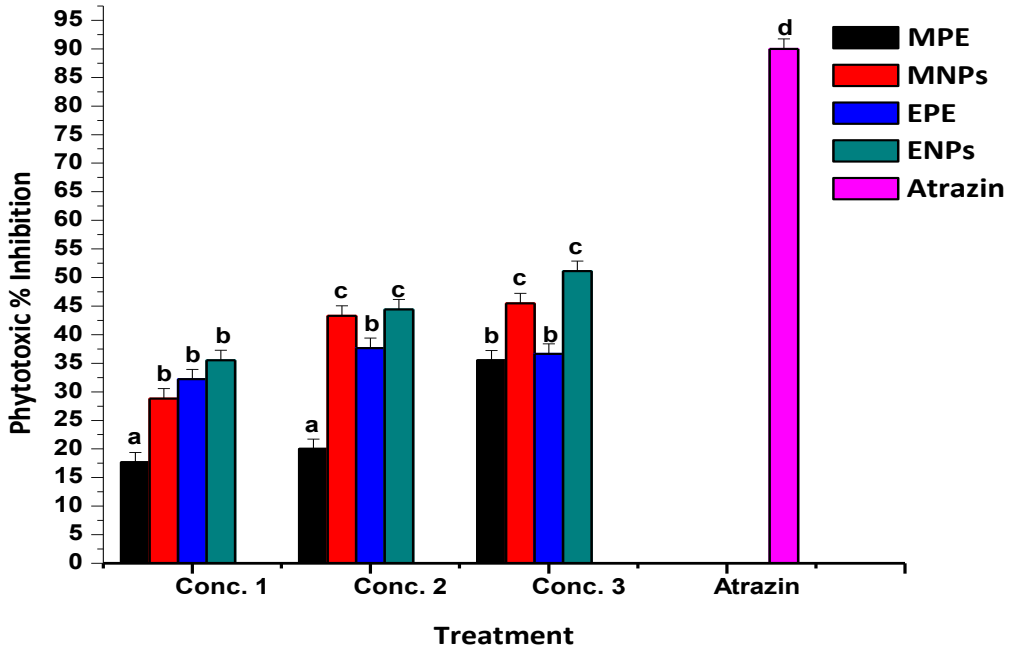

572

573 **Figure 13;** Phytotoxic activity of the methanolic extract-AgNPs, theextract-AgNPs, the ethanolic
574 extract-AgNPs, methanolic and ethanolic extract of *A. incisum* and Atrazin.

575

576 4.4.4. Anti-inflammatory activity

577 The anti-inflammatory potential was evaluated using methanolic and ethanolic extracts of
578 *A. incisum* along with their respective silver nanoparticles (AgNP) through the carrageenan-
579 induced paw edema technique in Swiss albino mice (**Figure 14**). The data obtained showed that
580 AgNPs derived from plant extracts were more effective than the extracts on their own. Aspirin,
581 the standard drug, showed exceptional anti-inflammatory activity by significantly (p<0.001)
582 inhibiting 87.5% of inflammation. Among the samples tested, those with the highest anti-
583 inflammatory activity were methanolic extract AgNP (MNP) which significantly inhibited 79.2%
584 of inflammation at 300 mg/kg. The MNPs were followed by methanolic plant extract (MPE),
585 which at the same concentration showed a significant (p>0.001) inhibition (p> 0.001) of 66.75%.

586

587 Ethanolic extract AgNP (ENP) showed highly significant (p<0.001) inhibition (p<0.001)
588 of 75% at a dose of 300 mg/kg while ethanolic plant extract (EPE) also showed a significant
589 (p<0.001) inhibition (p<0.001) of 70.8% at the same concentration.

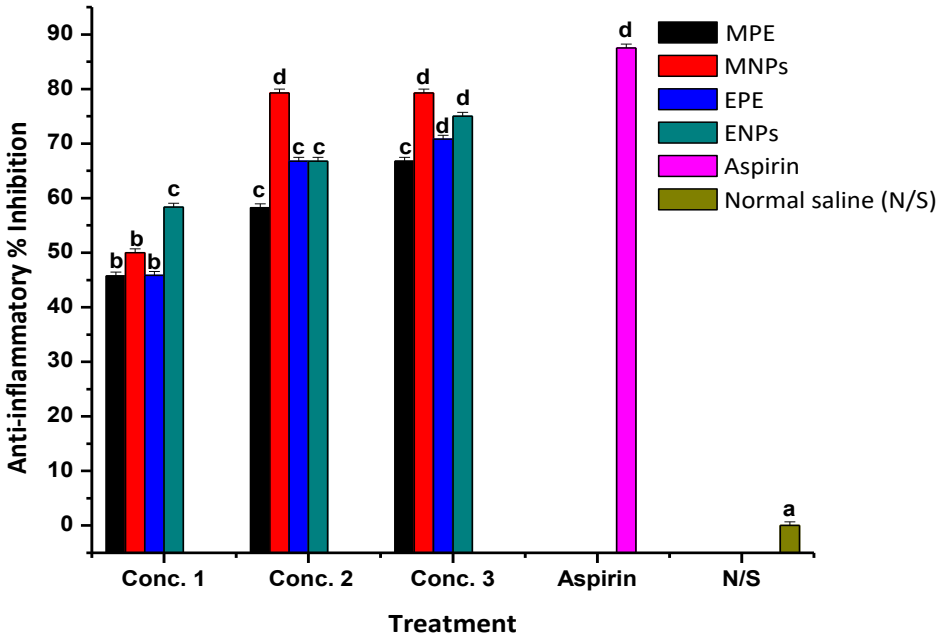

Figure 14: Anti-inflammatory activity of methanolic extract AgNP, ethanolic extract,-AgNPs, methanolic extract and ethanolic extract of *A. incisum* and Aspirin.

4.4.5. Analgesic Activity

The analgesic activities of the methanolic and ethanolic extracts of *A. incisum* along with the silver nanoparticles were studied (**Figure 15**). The data obtained showed that the analgesic activities of the synthesized nanoparticles were more effective than those of the plant extracts. The control drug paracetamol was the most potent analgesic drug with maximum activity significantly (p<0.001) inhibited 83.3% of inflammation at 500 µg/mL. Among the nanoparticles, ethanolic extract AgNPs (ENP) had the highest activity reaching 65.2% (p<0.001) at 500µg/mL. Furthermore, ethanolic plant extract (EPE) showed a significant (p<0.001) inhibition of 57.66% at 500 µg/mL. In comparison, AgNP methanolic extract (MNP) showed an inhibition rate of 61.11% (p<0.001) whereas, methanolic plant extract (MPE) exhibited a significant inhibition of 55.5% (p<0.001) at 500 µg/mL.

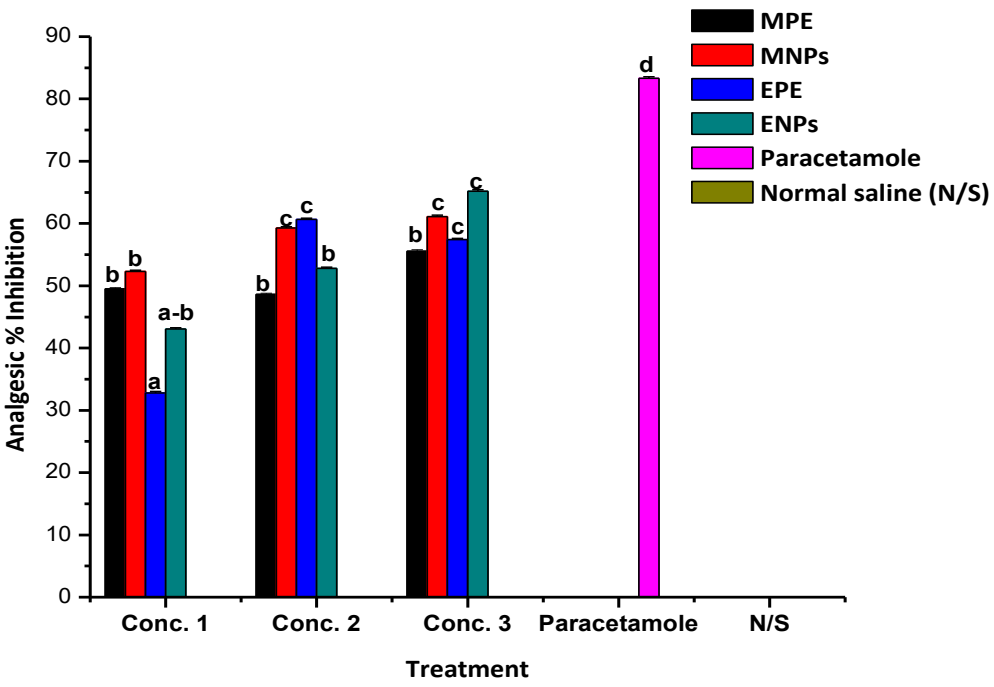

606

607 **Figure 15;** Analgesic activity of the methanolic extract-AgNPs, theextract-AgNPs, the ethanolic
608 extract-AgNPs, methanolic and ethanolic extract of *A. incisum* and paracetamol.

609

610

611 4.4.6. Antibacterial Activity

612 The antibacterial activities of A. incisum methanolic and ethanolic extracts, as well as their
613 biosynthesized silver nanoparticles (AgNP), were tested against *Shigella dysenteriae* (B1) and
614 *Pseudomonas aeruginosa* (B2) (**Figures 16 and 17**). The result revealed that AgNPs had
615 considerably larger zones of inhibition than the respective plant extracts. The highest activity was
616 displayed by the standard drug streptomycin (C^+), which caused a significant (p<0.0001) inhibition
617 zone (p<0.0001) of 24 mm against *S. dysenteriae* and 22 mm against *P. aeruginosa* followed by
618 the ethanolic extract-AgNP (ENP) showed highest significance (p<0.000) inhibition zone (p
619 <0.000) of 22 mm against *S. dysenteriae* at 100µL/mL and 20 mm against *Pseudomonas*
620 *aeruginosa* at 100µL/mL, In contrast, ethanolic plant extract (EPE) had a significant (p<0.028)
621 inhibition zone (p<0.028) of 16 mm against *P. aeruginosa* at a concentration of 100µL/mL, but
622 demonstrated a low significant 14 mm (p<0.484) inhibition zone against *S. dysenteriae*.

Similarly, methanolic extract nanoparticles (MNP) showed significant (p< 0.001) inhibition zone (p<0.001) of 18 mm at 100 µL/mL against *Pseudomonas aeruginosa* and 22 mm against *S. dysenteriae* at 100 µL/mL. On the other hand, methanolic plant extract (MPE) showed a significant (p<0.082) inhibition zone (p<0.082) of 12mm against *Pseudomonas aeruginosa* at 100µL/mL and 14mm against *Pseudomonas aeruginosa* at 100µL/mL.

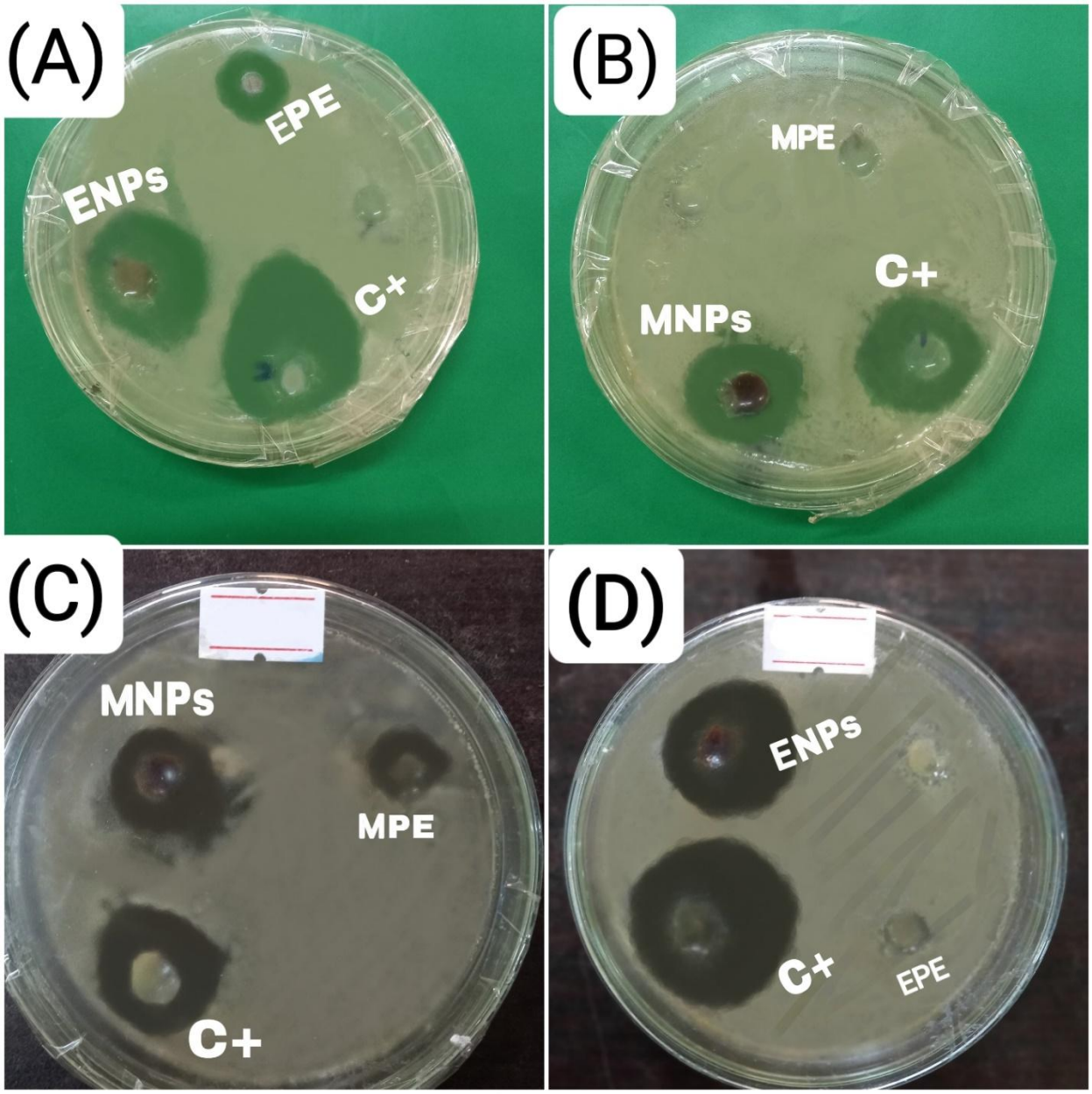

Figure 16: Antibacterial activity of methanolic and ethanolic extracts of AgNPs and plant extracts (methanolic and ethanolic) against *Shigella dysenteriae* (A) and (B) and *Pseudomonas aureginosa* (C) and (D).

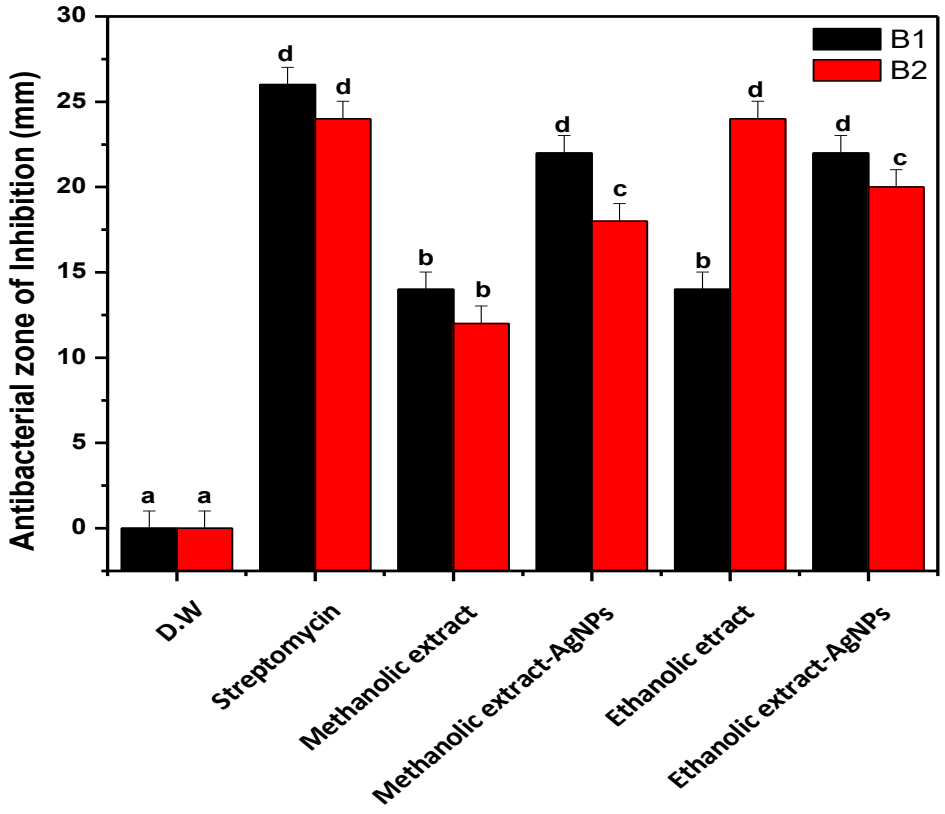

Figure 17: B1 represents *Shigella dysenteriae* and B2 represents *Pseudomonas aureginosa.*

4.4.7. Antifungal activity

The antifungal properties of silver nanoparticles (AgNP) biofabricated from methanolic and ethanolic extracts of *A. incisum* were evaluated using the well diffusion method **(Figure 18).** Evaluation of antifungal potential was done by checking the formation of inhibition zones at three different concentrations (25, 50, and 100 µL/mL). The standard antifungal drug clotrimazole (C+) exhibited the highest inhibition zone of 20 mm (p<0.001) against *Aspergillus niger* at 100 µL/mL. However, neither ethanolic plant extract (EPE) nor methanolic plant extracts (MPE) exhibited antifungal activity. Interestingly, methanolic extract nanoparticles (MNP) demonstrated remarkable inhibition zones of 14 mm (p<0.001) at 100 µL/mL and 11 mm at 50 µL/mL against

A. niger. Furthermore, the ethanolic extract nanoparticles (ENP) showed significant (p<0.001) inhibition zones (p<0.001) of 12 mm at 100 µL/mL and 10 mm at 50 µL/mL against *A. niger* **(Figure 19).**

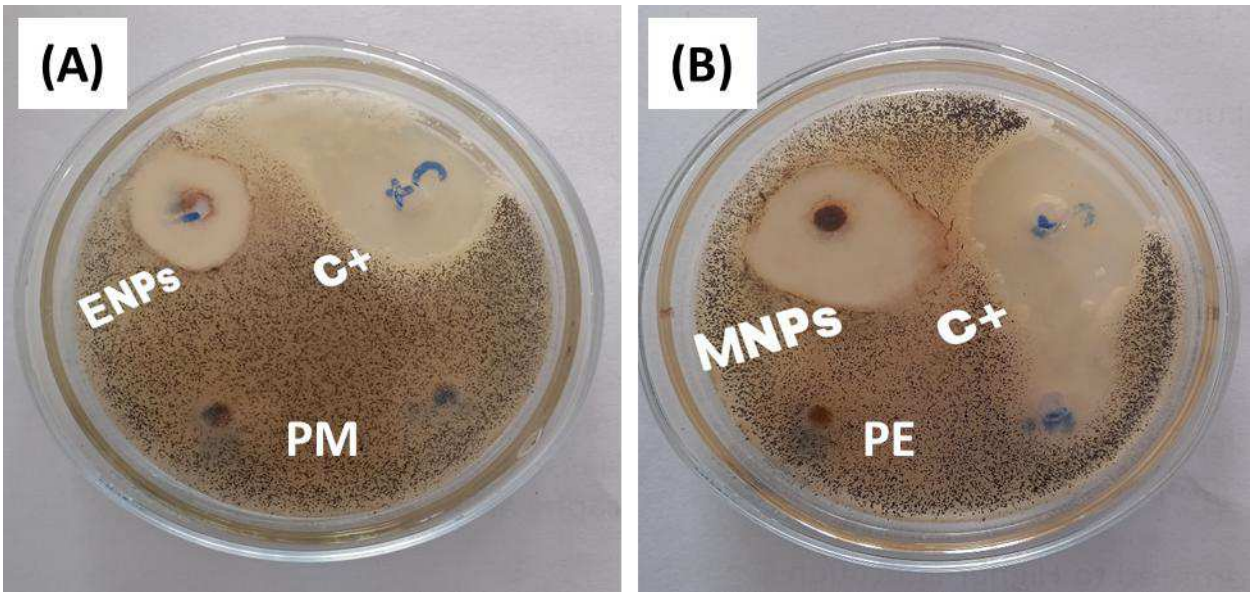

Figure 18: Antifungal activity of ethanolic extract extract (A) and methanolic extract extract-AgNP (B) against *Aspergillus niger*. Where C^+ indicates positive control, ENPs show ethanolic nanoparticles, MNPs show methanolic nanoparticles, PM shows methanol extract and PE shows ethanol extract, respectively.

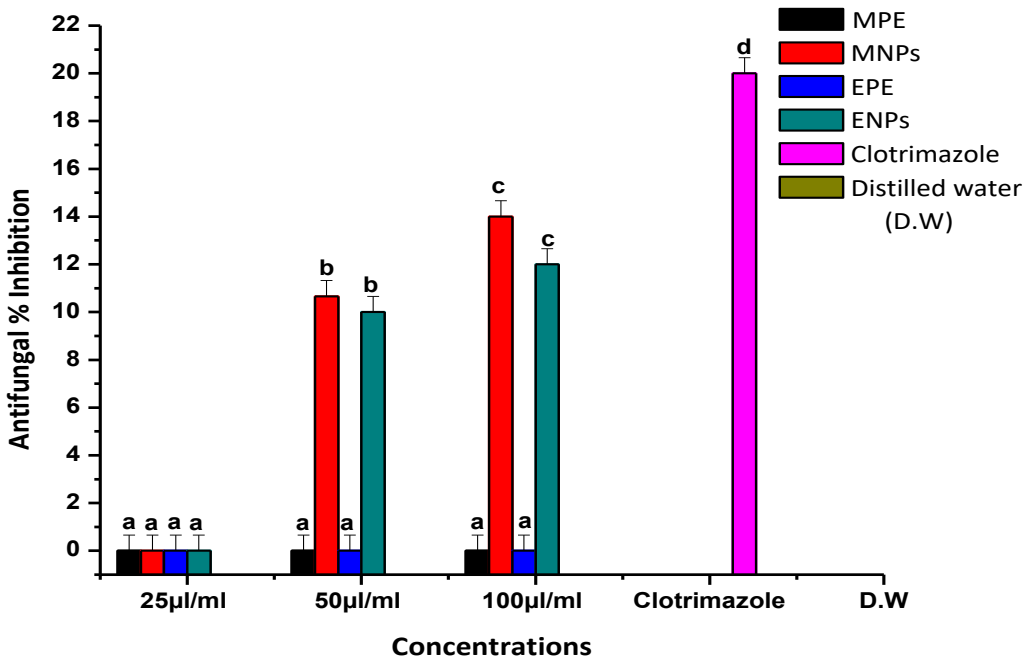

Figure 19: Antifungal activity of methanolic and ethanolic extract-AgNP, methanolic and ethanolic extracts of *A. incisum* and Clotrimazole.

5. Discussion

The synthesis of nanoparticles, especially green nanoparticles is a safer and eco-friendly approach that does not require the usage of toxic chemicals in their synthesis. This latest technology uses an array of metals for the synthesis of green nanoparticles; however, the use of aluminum (Ag) is more common, because of its easy synthesis, non-toxicity, cheaper, and easily characterizable. In the current study, we used *A. incisum* extracts (methanol and ethanol) for the biofabrication of AgNPs and its characterizations. The synthesis of Ag nanoparticles was first confirmed by changing the color of the solution from pale green to dark brown, according to previous findings (Begum et al., 2024). Similarly, different groups have used similar approaches, for example, (Hemlata et al., 2020) previously used *the* aqueous leaf extract and (Asghar et al., 2020) used the leaf extract of *Cymbopogon citratus.* They also noticed the synthesis of AgNPs and indicated that the solution color from light green and whitish to dark brown (Asad et al., 2022).

The synthesis of silver nanoparticles (AgNP) depends on different factors, among all, the pH of the reaction medium is a key factor (Ahmadi & Lackner, 2024). Interestingly, our results

indicated that AgNPs from *A. incisum* extracts (methanol and ethanol) were stable under different pH conditions; however, pH 9 was found to be suitable. Our results are consistent with the findings of (Murali Krishna et al., 2016), who evaluated the effect of pH variables on AgNP synthesis using *Asalmalia malabaric* and found that pH 9 was ideal for silver nanoparticle production. The size of the nanoparticles decreases due to the strong repulsive forces in colloidal solutions caused by the large concentration of OH (hydroxyl) groups on their surface at alkaline pH, which also minimizes particle aggregation (A. Ahmed et al., 2022).

AgNP size has been shown to be temperature dependent because the reaction temperature affects AgNP synthesis kinetics of AgNPs (Duman et al., 2024; M. B. Singh et al., 2024). The effects on the bio-fabrication of AgNPs from methanolic and ethanolic extracts of *A. incisum* were evaluated at a different temperature as previously reported previously (Nindawat & Agrawal, 2019). (L. Huang et al., 2020) worked on the biosynthesis of AgNPs using Ginkgo biloba leaf extract. They also studied the optimization of the temperature of the synthesized AgNPs, which showed an increase in absorption bands with increasing temperature from 40 to 60 ° C (Jamdagni et al., 2018).

The concentration of NaCl also greatly affects the controlled synthesis of silver nanoparticles of a particular size and shape (A. Ahmed et al., 2022). (Murali Krishna et al., 2016) and (Reduan et al., 2016), also demonstrated the biosynthesizing effects of NaCl on AgNP and showed the maximum absorbency at 5mM NaCl concentration of NaCl and 30mM NaCl respectively. Our findings align closely with those reported by (Asad et al., 2022), who investigated the impact of NaCl on the biosynthesis of AgNPs from *Amaryllis vittata*. Their results demonstrated that increasing the NaCl concentration from 0.2 to 1 mL caused a decrease in the absorbency peak, with the lowest absorbance measured at 1 mL of NaCl solution, and the highest peak wavelength noted at 0.2 mL.

AgNO3 concentration has a profound impact on AgNP synthesis of AgNPs (Othman et al., 2017). According to (Corciova & Ivanescu, 2018), the optimal ratio of plant extract to silver nitrate for AgNP synthesis was 1:5, achieved through a green methodology using *Tilia cordata*. This ratio guarantees the rapid and steady production of nanoparticles, as it produced the highest absorbance peak (M. Khan et al., 2018) optimized several constraints for biofabricating AgNPs with *Piper*

betle leaves. Their results showed that stable AgNPs were formed with 1: 4 aqueous leaf extract, 2 mM AgNO3 solution, and 9 pH (Begum et al., 2024).

The FTIR method is implemented for the detection of functional groups on the surface of silver nanoparticles (Mani et al., 2021). Our findings were very similar to the findings of (Acay, 2019) and (Dadashpour et al., 2018), who carried out FT-IR analysis on AgNPs from *Vitis vinifera* and *Matricaria chamomilla*, respectively. The findings of their study indicated that active reduction processes of the OH, -CN and C=O groups are be the causes of shifts at 3331, 2129, and 1612 cm-1 (Ullah et al., 2024) presented their research on FTIR analysis of AgNPs synthesized by *Peganum harmala* leaf extract. Their results showed that the presence of CH group is revealed by absorption band at 2927.36 cm-1. Furthermore, the FT-IR bands at 3397.10 and 3428.48 cm-1 were assigned to the assignments of OH groups. Bands at 1624.44 and 1606.44 cm-1 were assigned to the OC group of carboxylic acid, while bands at 1385.92 cm-1 and 1422.42 cm-1 were assigned to C–C group of alkenes. The absorption band between 1050 and 1200 cm-1 is due to the CO group of alcohols, ethers, and esters (Asad et al., 2022).

XRD characterization is employed for determining the crystalline structure of biofabricated AgNPs where atoms with crystal shapes lead to collision of X-ray beams which causes diffraction in several specific angles (Asghar et al., 2020). According to our findings, AgNPs exhibited crystallinity attributes, indicating that rays were developed within the lattice planes, while the broadened peak in the XRD analysis confirmed the existence of minuscule NPs and showed no signs for notable rests or contaminants (Keshari et al., 2020). (Aslam et al., 2021) conducted an XRD analysis of silver nanoparticles synthesized using the *Sanvitalia procumbens* extract. In their result, the XRD peaks appeared at 38, 45, and 64◦. These peaks correspond to planes 111, 200, and 220, respectively. XRD analysis was performed on AgNP produced with *Melia azedarach* leaf extract by (Jebril et al., 2020).

SEM analysis is used to assess and evaluate the form and surface characteristics of nanomaterials at various levels of magnification (Asad et al., 2022). (R. Khan et al., 2023)) Utilized SEM analysis was used to evaluate the morphology of AgNP synthesized by *Alocasia odora*. Their findings confirmed that the AgNPs had a spheroidal, irregular shape, and of different sizes. The SEM analysis of AgNPs was reported by (Bhat et al., 2021). The results proved that AgNPs showed a spherical, unevenly distributed, and somewhat aggregative shape in the SEM image. The reason for this adhesion is the high surface energy of the nanoparticles and the organic molecules

735 that cover their surface (Esmaile et al., 2020). The aggregation of silver nanoparticles was found
736 to occur when two or more reducing moieties bond to the surface of prepared nuclei (Surega et al.,
737 2020).
738 The presence of silver in synthesized nanomaterials is verified by using the EDS
739 technique (Safa & Koohestani, 2024). (Mofolo et al., 2020) created silver nanoparticles from
740 *Pechuel-loeschea leubnitzia* and used energy dispersive spectroscopy for elemental analysis.
741 These studies proved that biosynthesized AgNPs had silver together with oxygen, nitrogen, and
742 carbon. The results matched very closely with our study and prove that the existence of peaks of
743 other elements such as carbon, oxygen, and chlorine is the result of organic compounds that cover
744 the surface of the nanoparticles (Safa & Koohestani, 2024).
745
746 Numerous researches indicate that around two-thirds of the Earth's plant life has healing
747 properties especially the antioxidant effect of medicinal plants (Shehzada, 2018). (Mendam &
748 Naik, 2023) assessed the antioxidant potential of AgNP using *Galphimia glauca*. The silver
749 nanoparticles showed scavenging activity at concentrations of 100, 200, 400, 600, 800, and 1000
750 mg / ml, and their result showed inhibition of 48.75%, 53.48%, 59.19%, 67.05%, 74.1% and
751 77.67%, respectively. (Sharifi-Rad et al., 2021) screened AgNPs from *Otostegia persica* leaf
752 extract for its DPPH scavenging assay. The maximum antioxidant capacity achieved was 84 % at
753 a concentration of 300 µg/mL, while O. persica leaf extract produced an antioxidant activity of
754 64%. Functional groups present on the surface of AgNPs that reduce and limit the Ag+ ion possess
755 antioxidant potential (Keshari et al., 2020).
756 AgNPs can harm insects by penetrating their cell membranes (Deka et al., 2021; Rai et al.,
757 2018). (Vadlapudi & Amanchy, 2017) utilized silver nanoparticles from Myriostachya *wightiana*
758 against *Tribolium castaneum* to investigate the insecticidal efficacy of AgNP. Their results showed
759 55.2% mortality at a concentration of 150g. Similarly, (AS & S, 2019) reported work on the
760 insecticidal activity of AgNPs and in combination with malathion against *Tribolium castaneum*.
761 AgNPs alone demonstrated a 75% mortality rate, while malathion demonstrated a 95% mortality
762 rate. However, a death rate was noted when AgNPs and malathion were combined. Insect mortality
763 is associated with the surface expansion of the integument due to AgNP-induced dehydration.
764 Several plants and their derived nanoparticles (NP) act as herbicides as the secondary
765 metabolites of plants act as allelochemicals against hazardous plants (Sultana et al., 2019). The

phytotoxic capacity of AgNPs of *Euphorbia dracunculoides* was investigated by (Khattak et al., 2019) at concentrations of 10, 100 and 1000 µg/mL and demonstrated inhibition of 15.46%, 22.68% and 40.20%, respectively. whereas AgNPs showed inhibition of 21.6%, 46% and 69.0%. The creation of silver nanoparticles triggers certain stimulants, altering the biomass of the *Lemna plant* and disrupting photosynthesis, as well as chlorophyll formation (Dewez et al., 2018; Sultana et al., 2019).

Silver nanoparticles (AgNPs) are well known for their exceptional anti-inflammatory capabilities (Lu et al., 2025). Interestingly, AgNPs derived from *A. incisum* extracts (methanol and ethanol) showed significant anti-inflammatory potential in comparison to plant extracts. Our findings are closely aligned with (Jyoti et al., 2021), who reported the anti-inflammatory properties of AgNPs biofabricated from the extract of *Cassia fistula*. Their results revealed anti-inflammatory effects by achieving an inhibition range of 60-70%. Similarly, (Sati et al., 2020) studied the anti-inflammatory effects of AgNP fabricated from the leaves of *Ficus palmata* leaves. Their findings showed that the control drug diclofenac sodium recorded a stabilization of 93.55%, while AgNP at 2.5µL/mL had 79.89% inhibition. The ability of a plant to reduce inflammation directly depends on the presence of phytoconstituents, such as flavonoids, alkaloids, etc. However, AgNPs improve the capability of nanoparticles to act on cell and anti-inflammatory mechanisms (Agarwal et al., 2019).

Numerous studies have revealed the antianalgesic properties of AgNPs (Bozkaya et al., 2022; Chen et al., 2024; Chiguvare et al., 2016). Our results demonstrated that AgNPs derived from extracts of *A. incisum* (methanol and ethanol) presented a significant analgesic effect. Our results align with previous findings of (I. Khan et al., 2021), where they synthesized AgNPs from *Bunium persicum* revealed 90% analgesic potential and *B. persicum* extract had 70% inhibition at 300 ug / ml. In the same way, (Shah et al., 2017) investigated the analgesic properties of *Dryopteris blanfordii*. Their findings demonstrated 45% inhibition in contrast to 40.43% inhibition for the standard drug (aspirin).

In the field of nanomaterials, silver nanoparticles (AgNPs) have obtained interesting antibacterial properties (Bruna et al., 2021; Menichetti et al., 2023; Silva et al., 2017). In the current study, AgNPs derived from *A. incisum* extracts (methanol and ethanol) showed a significant antibacterial effect compared to plant extracts. It is interesting to note that, compared to standard drugs, ethanolic AgNPs caused interesting inhibition, followed by methanolic AgNPs and plant

extracts (without Ag). (Urnukhsaikhan et al., 2021) examined the antibacterial potential of Carduus *crispus* and noticed significant inhibitions, i.e. 6.5 ± 0.3 and 7.5 ± 0.3mm caused by AgNPs against *E. coli* and *M. luteus,* respectively.(Said et al., 2024) investigated the antibacterial properties of AgNPs from *Lawsonia inermis* against *Acinetobacter baumannii*, *Klebsiella pneumoniae*, *Escherichia coli*, *Enterococcus faecalis*, *Proteus mirabilis*, *Staphylococcus arlettae* and *Pseudomonas aeruginosa* and showed inhibitory zones of 30 ± 1.2, 28 ± 1.2, 27 ± 0.8, 26 ± 1.2, 25 ± 1.1, 19 ± 0.6 and 21 ± 0.9mm respectively.

Several researchers have demonstrated the antifungal effects of AgNPs (Saratale et al., 2018). In the current study, AgNPs derived from *A. incisum* extracts (methanol and ethanol) showed significant antifungal potential. Similar results were also reported by (Moond et al., 2023) who also synthesized AgNPs from leaf extract of *Trigonella foenum-graceum* L. Their findings demonstrated that AgNPs exhibited significant antifungal properties, exhibiting a maximum inhibition zone of 23 ± 0.17 mm against *Macrophomina phaseolina* and 22 ± 0.15 mm against *Fusarium oxysporum*. In the same way, (Arsene et al., 2023) reported the antifungal efficacy of AgNP biofabricated from Aloe vera extract against *Candida albicans;* however, the maximum inhibitory zone of AgNPs was 22 mm.

6. Conclusion

In this study, we successfully synthesized silver nanoparticles (AgNP) using methanolic and ethanolic extracts of *Adiantum incisum*, confirmed by a significant color change from bright green to dark brown and UV spectroscopy with absorbance peaks between 400-500nm. Similarly, optimizing biosynthesis parameters including temperature, pH, and salt concentrations enhanced AgNP production. In the same way, characterization through FTIR, XRD, EDX, and SEM showed functional groups included in capping and reduction, a face-centered cubic crystalline structure, monodispersed spherical particles, and the presence of elemental silver, respectively. Compared to plant ethanolic and methanolic extracts, AgNPS showed more interesting effects in different biological assays, such as insecticidal activity against *Tribolium castaneum*, phytotoxicity against *Lemna minor*, antioxidant activity through the DPHH assay, analgesic effect in acetic acid-induced writhing tests, anti-inflammatory efficacy in carrageenan-induced paw edema models, antibacterial activities against *Shigella dysenteriae* and *Pseudomonas aeruginosa* and antifungal potential against *Aspergillus niger*. Based on our findings, we suggest that the biosynthesized

AgNPs from *A. incisum* extracts hold significant potential for agricultural and pharmaceutical applications.

Consent to publish

Not applicable

Consent to participate

Not applicable

Data Availability Statement

The datasets generated during and/or analyzed during the current study are available from the corresponding author on reasonable request.

Competing interest

All authors declared that they had no competing interests.

Ethics declaration:

Not applicable.

Funding

The current study does not receive any funding.

Authors contribution

M. A. S and W. M Designed the project and conducted research activities. A. K, S. A. and H.A.B Analyzed the data. A.K, O.A.L, M. A. A, and B.S.M.A.K. Conceptualisation. O.A.L, M. A. A, and B.S.M.A.K. Formal analysis. M. A. S and W. M. A.K, O.A.L, M. A. A, and B.S.M.A.K. Investigation. S. A. and H.A.B. O.A.L, M. A. A and B.S.M.A.K. Methodology. A.K, O.A.L, M. A. A, and B.S.M.A.K. Drafted the very first manuscript. W. M Supervised the project and facilitated resources. All authors have read the article and agreed to submit it for publication.

Acknowledgment

The authors thank the Department of Botany for successfully completing the project. The authors are also thankful to the Fundação Coordenação de Aperfeiçoamento de Pessoal de Nível Superior (CAPES, Finance code 001) for the support.

References

Acay, H., 2019. Biosynthesis and characterization of silver nanoparticles using fig (Ficus carica) leaves: a potential antimicrobial activity. *Applied Ecology & Environmental Research.* 17(6).

Acay, H., Baran, M., & Eren, A., 2019. Investigating antimicrobial activity of silver nanoparticles produced through green synthesis using leaf extract of common grape (Vitis vinifera). *Applied Ecology & Environmental Research.* 17(2).

Agarwal, H., Nakara, A., & Shanmugam, V. K., 2019. Anti-inflammatory mechanism of various metal and metal oxide nanoparticles synthesized using plant extracts: A review. *Biomedicine & Pharmacotherapy.* 109, 2561-2572.

Ahmadi, F., & Lackner, M., 2024. Green synthesis of silver nanoparticles from Cannabis sativa: Properties, synthesis, mechanistic aspects, and applications. *ChemEngineering.* 8(4), 64.

Ahmed, A., Rauf, A., Hemeg, H. A., Qureshi, M. N., Sharma, R., Aljohani, A. S., . . . Rahman, M. M., 2022. Green synthesis of gold and silver nanoparticles using Opuntia dillenii aqueous extracts: characterization and their antimicrobial assessment. *Journal of Nanomaterials.* 2022(1), 4804116.

Ahmed, S., Ahmad, M., Swami, B. L., & Ikram, S., 2016. A review on plants extract mediated synthesis of silver nanoparticles for antimicrobial applications: a green expertise. *Journal of advanced research.* 7(1), 17-28.

Alharbi, N. S., Alsubhi, N. S., & Felimban, A. I., 2022. Green synthesis of silver nanoparticles using medicinal plants: Characterization and application. *Journal of Radiation Research and Applied Sciences.* 15(3), 109-124.

AP, S. K., 2024. Biosynthesis of Silver Nanoparticles using Histiopteris Incisa leaf extract and their Characterization and Thermophysical study. *Scientia Iranica*.

Arsene, M. M. J., Viktorovna, P. I., Alla, M., Mariya, M., Davares, A. K. L., Carime, B. Z., . . . Andreevna, S. L., 2023. Antimicrobial activity of phytofabricated silver nanoparticles using Carica papaya L. against Gram-negative bacteria. *Veterinary World.* 16(6), 1301.

AS, A. A., & S, T., 2019. Comparative bioassay of silver nanoparticles and malathion on infestation of red flour beetle, Tribolium castaneum. *The Journal of basic and applied zoology.* 80, 1-10.

Asad, S., Anwar, N., Shah, M., Anwar, Z., Arif, M., Rauf, M., . . . Albadrani, G. M., 2022. Biological synthesis of silver nanoparticles by Amaryllis vittata (L.) Herit: from antimicrobial to biomedical applications. *Materials.* 15(16), 5478.

Asghar, M., Habib, S., Zaman, W., Hussain, S., Ali, H., & Saqib, S., 2020. Synthesis and characterization of microbial mediated cadmium oxide nanoparticles. *Microscopy Research and Technique.* 83(12), 1574-1584.

Aslam, M., Fozia, F., Gul, A., Ahmad, I., Ullah, R., Bari, A., . . . Hussain, H., 2021. Phyto-extract-mediated synthesis of silver nanoparticles using aqueous extract of Sanvitalia procumbens, and characterization, optimization and photocatalytic degradation of azo dyes Orange G and Direct Blue-15. *Molecules.* 26(20), 6144.

Balamanikandan, T., Balaji, S., & Pandirajan, J., 2015. Biological Synthesis of silver nanoparticles by using onion (Allium cepa) extract and their antibacterial and antifungal activity. *World App Sci J.* 33(6), 939-943.

Begum, H. A., Yaseen, S., Zada, A., Musa, M., Khan, A., Sheheryar, . . . Azmat, R., 2024. Biological and Photocatalytic Activities of Silver Nanoparticles Synthesized from the Leaf Extract of Euphorbia royleana Boiss. *Current Pharmaceutical Design.* 30(35), 2813-2827.

Bhat, M., Chakraborty, B., Kumar, R. S., Almansour, A. I., Arumugam, N., Kotresha, D., . . . Nayaka, S., 2021. Biogenic synthesis, characterization and antimicrobial activity of Ixora brachypoda (DC) leaf extract mediated silver nanoparticles. *Journal of King Saud University-Science.* 33(2), 101296.

Bilal, H. M., Sharif, A., Malik, M. N. H., & Zubair, H. M., 2022. Aqueous ethanolic extract of Adiantum incisum Forssk. protects against type 2 diabetes mellitus via attenuation of α-amylase and oxidative stress. *ACS omega.* 7(42), 37724-37735.

Birla, S. S., Gaikwad, S. C., Gade, A. K., & Rai, M. K., 2013. Rapid synthesis of silver nanoparticles from Fusarium oxysporum by optimizing physicocultural conditions. *The Scientific World Journal.* 2013(1), 796018.

Bozkaya, O., Ekici, H., Gök, Z. G., Bozkaya, E., Ekici, S., Yiğitoğlu, M., & Vargel, İ., 2022. Investigation of the in vitro antibacterial, cytotoxic and in vivo analgesic effects of silver nanoparticles coated with Centella asiatica plant extract. *Ankara Üniversitesi Veteriner Fakültesi Dergisi.* 70(1), 87-96.

Bruna, T., Maldonado-Bravo, F., Jara, P., & Caro, N., 2021. Silver nanoparticles and their antibacterial applications. *International journal of molecular sciences.* 22(13), 7202.

Chen, H., Tian, C., & Zhang, L., 2024. Design and synthesis of dexmedetomidine capped silver nanoparticles: Investigation of its catalytic application for reduction of nitrobenzenes and its effects on anesthetic, anti-inflammatory, antioxidant and analgesic applications. *Journal of Organometallic Chemistry.* 1017, 123262.

Chick, C. N., Meva, F. E. a., Kedi, P. B. E., & Usuki, T., 2024. Green Synthesis of Silver Nanoparticles With Cyclosorus dentatus and Nephrolepis biserrata and Their Antioxidant, Anti-Inflammatory Studies. *Nano Select*, e202400093.

Chiguvare, H., Oyedeji, O. O., Matewu, R., Aremu, O., Oyemitan, I. A., Oyedeji, A. O., . . . Oluwafemi, O. S., 2016. Synthesis of silver nanoparticles using Buchu plant extracts and their analgesic properties. *Molecules.* 21(6), 774.

Chouhan, S., & Guleria, S., 2020. Green synthesis of AgNPs using Cannabis sativa leaf extract: Characterization, antibacterial, anti-yeast and α-amylase inhibitory activity. *Materials Science for Energy Technologies.* 3, 536-544.

Corciova, A., & Ivanescu, B., 2018. Biosynthesis, characterisation and therapeutic applications of plant-mediated silver nanoparticles. *Journal of the Serbian Chemical Society.* 83(5), 515-538.

Dadashpour, M., Firouzi-Amandi, A., Pourhassan-Moghaddam, M., Maleki, M. J., Soozangar, N., Jeddi, F., . . . Pilehvar-Soltanahmadi, Y., 2018. Biomimetic synthesis of silver nanoparticles using Matricaria chamomilla extract and their potential anticancer activity against human lung cancer cells. *Materials Science and Engineering: C.* 92, 902-912.

Das, K., Tiwari, R., & Shrivastava, D., 2010. Techniques for evaluation of medicinal plant products as antimicrobial agent: Current methods and future trends. *Journal of medicinal plants research.* 4(2), 104-111.

Das Purkayastha, M., & Manhar, A. K., 2016. Nanotechnological applications in food packaging, sensors and bioactive delivery systems. *Nanoscience in food and agriculture 2*, 59-128.

Deka, B., Babu, A., Baruah, C., & Barthakur, M., 2021. Nanopesticides: a systematic review of their prospects with special reference to tea pest management. *Frontiers in Nutrition.* 8, 686131.

Devi, A., Sharma, A., Sharma, H., Sharma, S., Raghuvanshi, P., & Shirkot, P., 2017. In vitro biosynthesis and characterization of bio silver nanoparticles of Pseudomonas putida LUA 15.1 and their potential as antibacterial agents. *Int J Chem Stud.* 5(4), 1817-1824.

Dewez, D., Goltsev, V., Kalaji, H. M., & Oukarroum, A., 2018. Inhibitory effects of silver nanoparticles on photosystem II performance in Lemna gibba probed by chlorophyll fluorescence. *Current plant biology.* 16, 15-21.

Duman, H., Eker, F., Akdaşçi, E., Witkowska, A. M., Bechelany, M., & Karav, S., 2024. Silver nanoparticles: A comprehensive review of synthesis methods and chemical and physical properties. *Nanomaterials.* 14(18), 1527.

Esmaile, F., Koohestani, H., & Abdollah-Pour, H., 2020. Characterization and antibacterial activity of silver nanoparticles green synthesized using Ziziphora clinopodioides extract. *Environmental nanotechnology, monitoring & management.* 14, 100303.

Farràs, A., Cásedas, G., Les, F., Terrado, E. M., Mitjans, M., & López, V., 2019. Evaluation of anti-tyrosinase and antioxidant properties of four fern species for potential cosmetic applications. *Forests.* 10(2), 179.

Femi-Adepoju, A. G., Dada, A. O., Otun, K. O., Adepoju, A. O., & Fatoba, O. P., 2019. Green synthesis of silver nanoparticles using terrestrial fern (Gleichenia Pectinata (Willd.) C. Presl.): characterization and antimicrobial studies. *Heliyon.* 5(4).

Gong, X., Jadhav, N. D., Lonikar, V. V., Kulkarni, A. N., Zhang, H., Sankapal, B. R., . . . Ma, Y., 2024. An overview of green synthesized silver nanoparticles towards bioactive antibacterial, antimicrobial and antifungal applications. *Advances in Colloid and Interface Science.* 323, 103053.

Hebbalalu, D., Lalley, J., Nadagouda, M. N., & Varma, R. S., 2013. Greener techniques for the synthesis of silver nanoparticles using plant extracts, enzymes, bacteria, biodegradable polymers, and microwaves. *ACS Sustainable Chemistry & Engineering.* 1(7), 703-712.

Hemlata, Meena, P. R., Singh, A. P., & Tejavath, K. K., 2020. Biosynthesis of silver nanoparticles using Cucumis prophetarum aqueous leaf extract and their antibacterial and antiproliferative activity against cancer cell lines. *ACS omega.* 5(10), 5520-5528.

Huang, H., Shan, K., Liu, J., Tao, X., Periyasamy, S., Durairaj, S., . . . Jacob, J. A., 2020. Synthesis, optimization and characterization of silver nanoparticles using the catkin extract of Piper longum for bactericidal effect against food-borne pathogens via conventional and mathematical approaches. *Bioorganic Chemistry.* 103, 104230.

Huang, L., Sun, Y., Mahmud, S., & Liu, H., 2020. Biological and environmental applications of silver nanoparticles synthesized using the aqueous extract of Ginkgo biloba leaf. *Journal of Inorganic and Organometallic Polymers and Materials.* 30, 1653-1668.

Ibrahim, S., Ahmad, Z., Manzoor, M. Z., Mujahid, M., Faheem, Z., & Adnan, A., 2021. Optimization for biogenic microbial synthesis of silver nanoparticles through response surface methodology, characterization, their antimicrobial, antioxidant, and catalytic potential. *Scientific Reports.* 11(1), 770.

Irfan, M., Jan, G., Jan, F. G., & Murad, W., 2021. Taxonomy and spore morphology of genus Adiantum (Vittarioideae; Pteridaceae) from Pakistan. *Microscopy Research and Technique.* 84(11), 2727-2736.

Jamdagni, P., Khatri, P., & Rana, J.-S., 2018. Green synthesis of zinc oxide nanoparticles using flower extract of Nyctanthes arbor-tristis and their antifungal activity. *Journal of King Saud University-Science.* 30(2), 168-175.

Jebril, S., Jenana, R. K. B., & Dridi, C., 2020. Green synthesis of silver nanoparticles using Melia azedarach leaf extract and their antifungal activities: In vitro and in vivo. *Materials Chemistry and Physics.* 248, 122898.

Jyoti, K., Arora, D., Fekete, G., Lendvai, L., Dogossy, G., & Singh, T., 2021. Antibacterial and anti-inflammatory activities of Cassia fistula fungal broth-capped silver nanoparticles. *Materials Technology.* 36(14), 883-893.

Keshari, A. K., Srivastava, R., Singh, P., Yadav, V. B., & Nath, G., 2020. Antioxidant and antibacterial activity of silver nanoparticles synthesized by Cestrum nocturnum. *Journal of Ayurveda and integrative medicine.* 11(1), 37-44.

Khan, I., Bawazeer, S., Rauf, A., Qureshi, M. N., Muhammad, N., Al-Awthan, Y. S., . . . Rengasamy, K. R., 2021. Synthesis, biological investigation and catalytic application using the alcoholic extract of Black Cumin (Bunium Persicum) seeds-based silver nanoparticles. *Journal of Nanostructure in Chemistry*, 1-19.

Khan, M., Tareq, F., Hossen, M., & Roki, M., 2018. Green synthesis and characterization of silver nanoparticles using Coriandrum sativum leaf extract. *Journal of Engineering Science and Technology.* 13(1), 158-166.

Khan, R., Naureen, H., Javed, A., Khalid, M., & Khan, H., 2023. Alocasia odora–mediated synthesis of silver nanoparticles, their cytotoxicity, and virucidal potential. *Applied Microbiology and Biotechnology.* 107(1), 111-123.

Khattak, U., Ullah, R., Khan, S., Afriq, S., Rauf, A., & Hassanien, M., 2019. Synthesis, characteristics and biological activities of silver nanoparticles from Euphorbia dracunculoides. *EurAsian Journal of BioSciences.* 13(2), 2249-2260.

Leo, B. F., Chen, S., Kyo, Y., Herpoldt, K.-L., Terrill, N. J., Dunlop, I. E., . . . Gow, A., 2013. The stability of silver nanoparticles in a model of pulmonary surfactant. *Environmental science & technology.* 47(19), 11232-11240.

Liu, Y., Wujisguleng, W., & Long, C., 2012. Food uses of ferns in China: a review. *Acta Societatis Botanicorum Poloniae.* 81(4).

Logeswari, P., Silambarasan, S., & Abraham, J., 2013. Ecofriendly synthesis of silver nanoparticles from commercially available plant powders and their antibacterial properties. *Scientia Iranica.* 20(3), 1049-1054.

Lu, J., Zhang, M., El-kott, A. F., AlShehri, M. A., Negm, S., & AlSheri, A. S., 2025. Supported silver nanoparticles over starch-modified magnetic nanoparticles: Characterization, Its application for A3 coupling reactions, analgesic and anesthetic activities. *Journal of Organometallic Chemistry*, 123544.

Mani, M., Pavithra, S., Mohanraj, K., Kumaresan, S., Alotaibi, S. S., Eraqi, M. M., . . . Kaviyarasu, K., 2021. Studies on the spectrometric analysis of metallic silver nanoparticles (Ag NPs) using Basella alba leaf for the antibacterial activities. *Environmental Research.* 199, 111274.

Mathew, M., & Paul, R. R. (2024). Nanofibers and Nanotechnology in Porous Textiles. In *Mechanics and Physics of Porous Materials* (pp. 237-253): Apple Academic Press.

Mendam, K., & Naik, S. J. K., 2023. Anticancer and antioxidant activities of Cyphostemma auriculatum Roxb. green mediated silver nanoparticles. *Materials Today: Proceedings.* 92, 618-625.

Menichetti, A., Mavridi-Printezi, A., Mordini, D., & Montalti, M., 2023. Effect of size, shape and surface functionalization on the antibacterial activity of silver nanoparticles. *Journal of Functional Biomaterials.* 14(5), 244.

Mofolo, M. J., Kadhila, P., Chinsembu, K. C., Mashele, S., & Sekhoacha, M., 2020. Green synthesis of silver nanoparticles from extracts of Pechuel-loeschea leubnitziae: their anti-proliferative activity against the U87 cell line. *Inorganic and Nano-Metal Chemistry.* 50(10), 949-955.

Moodley, J. S., Krishna, S. B. N., Pillay, K., Sershen, f., & Govender, P., 2018. Green synthesis of silver nanoparticles from Moringa oleifera leaf extracts and its antimicrobial potential. *Advances in Natural Sciences: Nanoscience and Nanotechnology.* 9(1), 015011.

Moond, M., Singh, S., Sangwan, S., Rani, S., Beniwal, A., Rani, J., . . . Devi, P., 2023. Phytofabrication of silver nanoparticles using trigonella foenum-graceum L. Leaf and evaluation of its antimicrobial and antioxidant activities. *International Journal of Molecular Sciences.* 24(4), 3480.

Murali Krishna, I., Bhagavanth Reddy, G., Veerabhadram, G., & Madhusudhan, A., 2016. Eco-friendly green synthesis of silver nanoparticles using Salmalia malabarica: synthesis, characterization, antimicrobial, and catalytic activity studies. *Applied Nanoscience.* 6, 681-689.

Narayanan, K. B., & Sakthivel, N., 2011. Green synthesis of biogenic metal nanoparticles by terrestrial and aquatic phototrophic and heterotrophic eukaryotes and biocompatible agents. *Advances in colloid and interface science.* 169(2), 59-79.

Nasrollahzadeh, M., Sajadi, S. M., Sajjadi, M., & Issaabadi, Z. (2019). An introduction to nanotechnology. In *Interface science and technology* (Vol. 28, pp. 1-27): Elsevier.

Nindawat, S., & Agrawal, V., 2019. Fabrication of silver nanoparticles using Arnebia hispidissima (Lehm.) A. DC. root extract and unravelling their potential biomedical applications. *Artificial cells, nanomedicine, and biotechnology.* 47(1), 166-180.

Othman, A. M., Elsayed, M. A., Elshafei, A. M., & Hassan, M. M., 2017. Application of response surface methodology to optimize the extracellular fungal mediated nanosilver green synthesis. *Journal of Genetic Engineering and Biotechnology.* 15(2), 497-504.

Panahi, H. K. S., Hosseinzadeh-Bandbafha, H., Dehhaghi, M., Orooji, Y., Mahian, O., Shahbeik, H., . . . Jouzani, G. S., 2024. Nanotechnology applications in biodiesel processing and production: A comprehensive review. *Renewable and Sustainable Energy Reviews.* 192, 114219.

Pandey, A., Tripathi, S., Kumar, B., Singh, P., Singh, H., Shukla, A. N., & Garg, A., 2024. Spore morphology of Adiantum species from the Indian subcontinent using LM and FESEM: palaeoecological analysis and phylogenetic delineation. *Palynology*, 2427638.

Patil, S., Lavate, R., Raole, V., & Rajput, K., 2022. Adiantum L.: overview on taxonomy, distribution, conservation status, ethnomedicinal uses, phytochemistry, and pharmacognosy from India. *Ferns: Biotechnology, Propagation, Medicinal Uses and Environmental Regulation*, 553-570.

Rafique, M., Sadaf, I., Rafique, M. S., & Tahir, M. B., 2017. A review on green synthesis of silver nanoparticles and their applications. *Artificial cells, nanomedicine, and biotechnology.* 45(7), 1272-1291.

Rai, M., Ingle, A. P., Pandit, R., Paralikar, P., Shende, S., Gupta, I., . . . da Silva, S. S., 2018. Copper and copper nanoparticles: Role in management of insect-pests and pathogenic microbes. *Nanotechnology Reviews.* 7(4), 303-315.

Rashidi, M. A., Falahi, S., Farhang Dehghan, S., Ebrahimzadeh, H., Ghaneialvar, H., & Zendehdel, R., 2024. Green synthesis of silver nanoparticles by Smyrnium cordifolium plant and its application for colorimetric detection of ammonia. *Scientific Reports.* 14(1), 24161.

Reddy, A., & Day, I. S. (2001). Cell cycle regulation in plants. In *Handbook of plant and crop physiology* (pp. 251-286): CRC Press.

Reduan, N. A., Ghazali, S., & Jamari, S. S., 2016. Effect of temperature and NaCl concentration on synthesis of silver nanoparticles prepared in aqueous medium. *ARPN J Eng Appl Sci.* 11(10), 6399-6404.

Safa, M. A. T., & Koohestani, H., 2024. Green synthesis of silver nanoparticles with green tea extract from silver recycling of radiographic films. *Results in Engineering.* 21, 101808.

Sahni, G., Panwar, A., & Kaur, B., 2015. Controlled green synthesis of silver nanoparticles by Allium cepa and Musa acuminata with strong antimicrobial activity. *International Nano Letters.* 5, 93-100.

Said, A., Abu-Elghait, M., Atta, H. M., & Salem, S. S., 2024. Antibacterial activity of green synthesized silver nanoparticles using Lawsonia inermis against common pathogens from urinary tract infection. *Applied Biochemistry and Biotechnology.* 196(1), 85-98.

Saratale, R. G., Benelli, G., Kumar, G., Kim, D. S., & Saratale, G. D., 2018. Bio-fabrication of silver nanoparticles using the leaf extract of an ancient herbal medicine, dandelion (Taraxacum officinale), evaluation of their antioxidant, anticancer potential, and antimicrobial activity against phytopathogens. *Environmental Science and Pollution Research.* 25, 10392-10406.

Sarella, P. N. K., Vegi, S., Vendi, V. K., Vipparthi, A. K., & Valluri, S., 2024. Exploring Aquasomes: A promising frontier in nanotechnology-based drug delivery. *Asian Journal of Pharmaceutical Research.* 14(2), 153-161.

Sarsar, V., Selwal, M. K., & Selwel, K. K., 2014. Significant parameters in the optimization of biosysnthesis o silver nanoparticles using Psidium guajava leaf extract and evaluation of their antimicrobial activity against human pathogenic bacteria. *Int J Adv Pharma Sci.* 5(1), 1769-1775.

Sati, S. C., Kour, G., Bartwal, A. S., & Sati, M. D., 2020. Biosynthesis of metal nanoparticles from leaves of Ficus palmata and evaluation of their anti-inflammatory and anti-diabetic activities. *Biochemistry.* 59(33), 3019-3025.

Shah, P. K., Santella, A., Jacobo, A., Siletti, K., Hudspeth, A., & Bao, Z., 2017. An in toto approach to dissecting cellular interactions in complex tissues. *Developmental cell.* 43(4), 530-540. e534.

Shahzadi, K., Bashir, F., Nazir, K., Seemab, S., Shaker, M. A. A., Waheed, I., . . . Fatima, K., 2019. Impacts of green synthesized Silver-Nanoparticles against Tribolium castaneum (Coleoptera: Tenebrionidae). *Int. J. Entomol. Res.* 4(6), 114-117.

Sharifi-Rad, M., Pohl, P., & Epifano, F., 2021. Phytofabrication of silver nanoparticles (Agnps) with pharmaceutical capabilities using otostegia persica (burm.) boiss. leaf extract. *Nanomaterials.* 11(4), 1045.

Sharma, A., Mittal, V., Grover, R., Sharma, D., Gupta, V., & Kumar, K., 2024. Applications of nanotechnology in phytoremediation. *Phytoremediation: Biological Treatment of Environmental Pollution*, 291-313.

Shehzada, S., 2018. Biological evaluation of efficacy of Aloe barbadensis L. extract. *Education.* 2021.

Silva, L. P., Silveira, A. P., Bonatto, C. C., Reis, I. G., & Milreu, P. V. (2017). Silver nanoparticles as antimicrobial agents: Past, present, and future. In *Nanostructures for antimicrobial therapy* (pp. 577-596): Elsevier.

Simpa, P., Solomon, N. O., Adenekan, O. A., & Obasi, S. C., 2024. Nanotechnology's potential in advancing renewable energy solutions. *Engineering Science & Technology Journal.* 5(5), 1695-1710.

Singh, M. B., Thakur, G., Raman, A. P. S., Singh, P., Kumar, P., Singh, R., . . . Kumari, K., 2024. A time and temperature dependent biosynthesis of silver nanoparticles using the extract of Platycladus orientalis' fruit. *Next Research.* 1(1), 100005.

Singh, R., 2019. Nanotechnology based therapeutic application in cancer diagnosis and therapy. *3 Biotech.* 9(11), 415.

Sultana, K., Ahmad, B., Rauf, A., Huang, L., & Ramadan, M. F., 2019. Synthesis, characterization and pharmacological activities of silver nanoparticles using Bistorta affinis and Malcolmia cabulica extracts. *Bioinspired, Biomimetic and Nanobiomaterials.* 9(1), 7-15.

Surega, R., Anita, B., Ramakrishnan, S., Gunasekaran, K., & Nakkeran, S., 2020. Synthesis and characterization of AgNps using plant extracts. *Int. J. Curr. Microbiol. Appl. Sci.* 9, 1939-1947.

Ullah, I., Rauf, A., Khalil, A. A., Luqman, M., Islam, M. R., Hemeg, H. A., . . . Quradha, M. M., 2024. Peganum harmala L. extract-based Gold (Au) and Silver (Ag) nanoparticles (NPs): Green synthesis, characterization, and assessment of antibacterial and antifungal properties. *Food Science & Nutrition.* 12(6), 4459-4472.

Urnukhsaikhan, E., Bold, B.-E., Gunbileg, A., Sukhbaatar, N., & Mishig-Ochir, T., 2021. Antibacterial activity and characteristics of silver nanoparticles biosynthesized from Carduus crispus. *Scientific reports.* 11(1), 21047.

Vadlapudi, V., & Amanchy, R., 2017. Phytofabrication of silver nanoparticles using Myriostachya wightiana as a novel bioresource, and evaluation of their biological activities. *Brazilian Archives of Biology and Technology.* 60, e17160329.

Vijayan, S. R., Santhiyagu, P., Ramasamy, R., Arivalagan, P., Kumar, G., Ethiraj, K., & Ramaswamy, B. R., 2016. Seaweeds: A resource for marine bionanotechnology. *Enzyme and microbial technology.* 95, 45-57.

Wang, Q., Shan, C., Zhang, P., Zhao, W., Zhu, G., Sun, Y., . . . Rui, Y., 2024. The combination of nanotechnology and potassium: applications in agriculture. *Environmental Science and Pollution Research.* 31(2), 1890-1906.